UNIVERSITY
OF GÄVLE

DEPARTMENT OF TECHNOLOGY AND BUILT ENVIRONMENT

Development of a MATLAB Simulation Environment for Vehicle-to-Vehicle and Infrastructure Communication Based on IEEE 802.11p

Samaneh Shooshtary

Vienna, December 2008

Master's Thesis in Telecommunications

Examiner: Prof. Claes Beckman

Supervisors: Univ.-Prof. Dipl.-Ing. Dr.-Ing. Christoph F. Mecklenbräuker

Dipl.-Ing. Alexander Paier

INSTITUT FÜR
NACHRICHTENTECHNIK UND
HOCHFREQUENZTECHNIK

TECHNISCHE
UNIVERSITÄT
WIEN

VIENNA
UNIVERSITY OF
TECHNOLOGY

Abstract

This thesis describes the simulation of the proposed IEEE 802.11p Physical layer (PHY). A MATLAB simulation is carried out in order to analyze baseband processing of the transceiver. Orthogonal Frequency Division Multiplexing (OFDM) is applied in this project according to the IEEE 802.11p standard, which allows transmission data rates from 3 up to 27 Mbps. Distinct modulation schemes, Binary Phase Shift Keying (BPSK), Quadrate Phase Shift Keying (QPSK) and Quadrature Amplitude modulation (QAM), are used according to differing data rates. These schemes are combined with time interleaving and a convolutional error correcting code. A guard interval is inserted at the beginning of the transmitted symbol in order to reduce the effect of Intersymbol Interference (ISI). The Viterbi decoder is used for decoding the received signal. Simulation results illustrate the Bit Error Rate (BER), Packet Error Rate (PER) for different channels. Different channel implementations are used for the simulations. In addition a ray-tracing based software tool for modelling time variant vehicular channels is integrated into SIMULINK. BER versus Signal to Noise Ratio (SNR) statistics are as the basic reference for the physical layer of the IEEE 802.11p standard for all vehicular wireless network simulations.

Acknowledgment

I would like to offer my heartfelt thanks to Professor Christoph F. Mecklenbräuker the principal supervisor providing me with support during the thesis. I also hereby offer my special gratitude to Alexander Paier, my supervisor at Technical University of Vienna who provided me with the facilities and data and scientific assistants. My thanks are also due to Professor Claes Beckman my examiner and teacher. My appreciation and thanks go to Rene Wahl, from AWE Communications company who always welcomed my questions with the best possible hints and helps.

Dedicated to :

My Parents; *Ali and Azam*

And to my husband Mahdi

Abbreviation

AWGN	Additive White Gaussian Noise
ACK	Acknowledgment
BER	Bit Error Rate
BPSK	Binary Phase Shift Keying
CTS	Clear to Send
CSMA	Carrier Sense Multiple Access
CDF	Cumulative Distribution Function
FFT	Inverse Fast Fourier Transformation
GI	Guard Interval
IFFT	Fast Fourier Transformation
ITS	Intelligent Transport Systems
IFS	Inter Frame Space
ISI	Intersymbol Interference
LOS	Line of Sight
MAC	Medium Access Control
NAV	Network Allocation Vector
OFDM	Orthogonal Frequency Division Multiplexing
OSI	Open System Interconnection
PER	Packet Error Rate
PHY	Physical layer
PDF	Probability Density Functions
PN	Pseudorandom Noise
QPSK	Quadrate Phase Shift Keying
QAM	Quadrature Amplitude modulation
RMS	Root Mean square
RTS	Request to send
SNR	Signal to Noise Ratio
V2V	Vehicle-to-Vehicle
V2I	Vehicle-to-Infrastructure

Contents

Chapter 1

Introduction

1.1 Motivation for Vehicular WLAN Connections

Vehicular communication system is a communication network which vehicles and roadside units are communicating with each other. The transferred information in this type of communication is warning messages and traffic information. Vehicular communication systems are effective in decreasing the accidents and traffic congestions. Due to the importance of road safety in recent years, the research on Vehicle-to-Vehicle (V2V) and Vehicle-to-Infrastructure (V2I) communication is increasing. IEEE 802.11p defines an international standard for wireless access in vehicular environments. Generally wireless access in vehicular environments contains two distinct types of networking which are V2V and V2I. Vehicular communications is categorized as a part of Intelligent Transport Systems (ITS). In addition, Vehicular communication networks will offer a wide range of applications such as providing traffic management with a real time data for responding to road congestions. In the other hand finding a better path by access to the real time data can be as the other advantage of vehicular communication system which cause saving the time and fuel and has large economic benefits. But road safety is the main goal of this network.

1.2 Overview

IEEE 802.11a is provided for indoor environment with high data rate communication and low user mobility. IEEE 802.11p is designed for operating at high user mobility (vehicular communication). In this thesis an existing IEEE 802.11a PHY Simulink, [1], is updated to obtain a 802.11p PHY model. Decreasing of the signal bandwidth from 20 MHz to 10 MHz in IEEE 802.11p makes the communication more efficient for high mobility vehicular channel such as reducing ISI caused by multipath channel with using doubled guard interval. This means that the parameters in the time domain are doubled, compare with the parameters from IEEE 802.11a [2].

For studying the Medium Access Control (MAC) and higher layers of communication systems, the lower layer (PHY) and wireless channel have to be considered due to their significant effect on the computational efficiency and the correctness of simulation results. The draft IEEE 802.11p standard defines a MAC and a PHY based on OFDM technique for future vehicular communication devices. But, the study on the specification of a IEEE 802.11p PHY working in high mobility environments has the potential to be improved. The main goal of this thesis is the evaluation of V2V and V2I communication PHY based on IEEE 802.11p standard by MATLAB Simulations. In this work we refer to the BER versus SNR statistics that can be used as the basic reference for the physical layer of the IEEE 802.11 p standard for all vehicular wireless network simulations. In order to get realistic simulation results, a special radio channel simulator is used. This channel simulator is called WinProp, [3], and is based on ray tracing. With this simulator time variant scenarios can be modelled. A description of the principles of the IEEE 802.11p PHY and working experience with MATLAB SIMULINK and WinProp software is explained in this thesis. This thesis is organized as follows: Section 1 is motivation for vehicular WLAN connection and principle of OFDM transmission. Section 2 provides properties of WLAN according to IEEE 802.11p. Section 3 describes a MATLAB SIMULINK model in software that includes transmitter, receiver and channel models. Section 4 defines the vehicular scenario in same direction and opposite direction. Section 5 is discussion of simulation results. Section 6 summarizes the thesis and presents conclusions.

1.3 Fading Statistics in Vehicular Mobile Channel

Fading occurs due to the multi-path propagation in communications systems.

As a result signals reach the receiver from several different paths that may have different lengths corresponding to different time delays and gains. Time delay causes additional phase shifts to the main signal component. Therefore the signal reaching the receiver is the sum of some copies of the original signal with different delays and gains. With this explanation, the channel impulse response can be modelled as described in [4] with

$$h_c(t) = \sum_{k=0}^{K-1} \alpha_k \delta(t - \tau_k). \tag{1.1}$$

α_k =Complex path gain

k =Number of paths

τ_k = Path delay

Two different scales of fading have been defined, large scale fading and small scale fading. Small scale fading happens in very short time duration and is caused by reflectors and scatters that change the amplitude, phase and angle of the arriving signal. Rayleigh distribution and Rician distribution are often used to define small scale fading. Large scale fading is due to shadowing and the mobile station should move over a large distance to overcome the effects of shadowing. To define large scale fading, log-normal distribution is often used. Figure 1.1 shows a scenario with multipath fading.

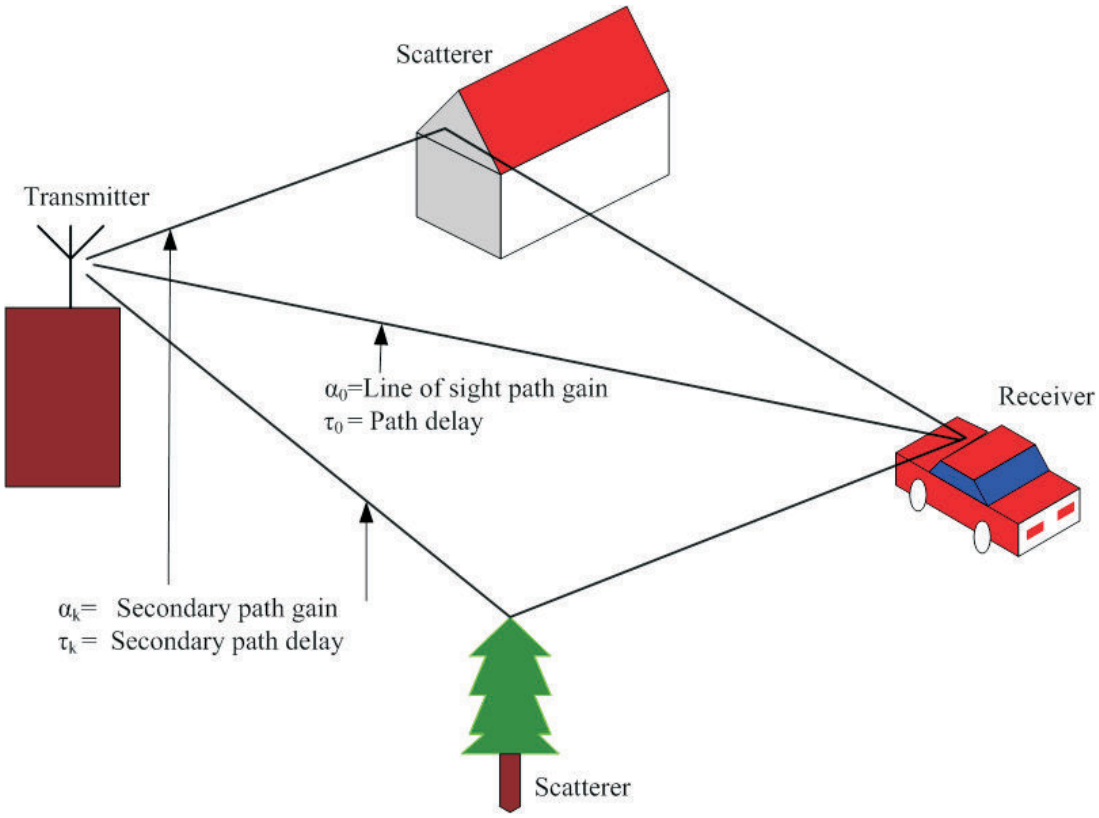

Figure 1.1: Multipath propagation.

1.3.1 Rayleigh Fading Distribution

Rayleigh distributions are defined for fading of a channel when all the received signals are reflected signals and there is no dominant component. The Rayleigh distributions has a Probability Density Functions (PDF) given by, [5],

$$p(r) = \begin{cases} \frac{r}{\sigma^2} exp\left(-\frac{r^2}{2\sigma^2}\right) & (0 \leq r) \\ 0 & (r < 0) \end{cases}, \tag{1.2}$$

where σ is the Root Mean Square (RMS) value of voltage in a received signal , and σ^2 is the time-average power of the received signal. The Cumulative Distribution Function (CDF) is defined to specify the probability that the received signal does not exceed a specific threshold R. The CDF is given by, [5],

$$P(R) = P(r \leq R) = \int_0^R p(r)dr = 1 - exp\left(-\frac{R^2}{2\sigma^2}\right). \tag{1.3}$$

1.3.2 Rician Fading Distribution

Rician fading distribution is applied in the case that a Line of Sight (LOS) component exists between the transmitter and the receiver. The Rician distribution is given by, [5],

$$p(r) = \begin{cases} \frac{r}{\sigma^2} exp^{\frac{-(r^2+A^2)}{2\sigma^2}} I_0\left(\frac{A_r}{\sigma^2}\right) & (A \geq 0, r \geq 0) \\ 0 & (r < 0) \end{cases}, \tag{1.4}$$

The A is the amplitude of the dominant component,σ is the RMS value of voltage in a received signal,σ^2 is the time-average power of the received signal and $I_0(.)$ is the modified Bessel function of the first kind and zero-order. Tke parameter K in Rician distribution is the ratio between the power of the LOS component and the disperse component,

$$K(\text{dB}) = 10\log\frac{A^2}{2\sigma^2} \qquad \text{dB} \tag{1.5}$$

Rayleigh distribution is one kind of Rician distribution for $K \to 0$. For $K >> 1$ the Rician distribution can be approximated by a Gaussian distributation, [5].

1.3.3 Log-Normal Distribution

Large scale fading is due to shadowing. In this case one possibility is to use a log-normal distribution function to define large scale fading of the channel. The log-normal distribution has a probability density function that is given by, [6],

$$f(r;\mu,\sigma) = \begin{cases} \frac{exp^{-(lnx-\mu)^2/2\sigma^2}}{x\sigma\sqrt{2\pi}} & (r \geq 0) \\ 0 & (r < 0) \end{cases}, \tag{1.6}$$

where μ is the mean deviation and σ is standard deviation of the variable's logarithm [6].

1.4 Principle of OFDM Transmission

Orthogonal Frequency Division Multiplexing (OFDM) is a multiplexing technique that divides a channel with a higher relative data rate into several orthogonal sub-channels with a lower data rate.

For high data rate transmissions,the symbol duration T_s is short. Therefore ISI due to multipath propagation distorts the received signal, if the symbol duration T_s is smaller as the maximum delay of the channel. To mitigate this effect a narrowband channel is needed, but for high data rates a broadband channel is needed. To overcome this problem the total bandwidth can be split into several parallel narrowband subcarriers. Thus a block of N serial data symbols with duration T_s is converted into a block of N parallel data symbols, each with duration $T = N \times T_s$. The aim is that the new symbol duration of each subcarrier is larger than the maximum delay of the channel, $T > T_{max}$. With many low data rate subcarriers at the same time, a higher data rate is achieved.

In order to create the OFDM symbol a serial to parallel block is used to convert N serial data symbols into N parallel data symbols. Then each parallel data symbol is modulated with a different orthogonal frequency subcarriers, and added to an OFDM symbol, [4].

1.4.1 Using Inverse FFT to Create the OFDM Symbol

All modulated subcarriers are added together to create the OFDM symbol. This is done by an Inverse Fast Fourier Transformation (IFFT). The advantage of using IFFT is that the system does not need N oscillators to transmit N subcarriers.

1.4.2 Cyclic Prefix Insertion

The cyclic prefix is used in OFDM signals as a guard interval and can be defined as a copy of the end symbol that is inserted at the beginning of each OFDM symbol. Guard interval is applied to mitigate the effect of ISI due to the multipath propagation.

Figure 1.2 shows the symbol and its delay. These delay make noise and distort the beginning of the next symbol as shown.

To overcome this problem, one possibility is to shift the second symbol furthers away from the first symbol. But existence of a blank space for a continuous communication system is not desired. In order to solve this problem a copy of the last part of the symbol is inserted at the beginning of each symbol. This procedure is called adding a cyclic prefix. Figure 1.3 shows the insertion of a cyclic prefix. The Cyclic prefix is added after the IFFT at the transmitter, and at the receiver the cyclic prefix is removed in order to get the original signal. A detailed mathematical explanation can be found in [4].

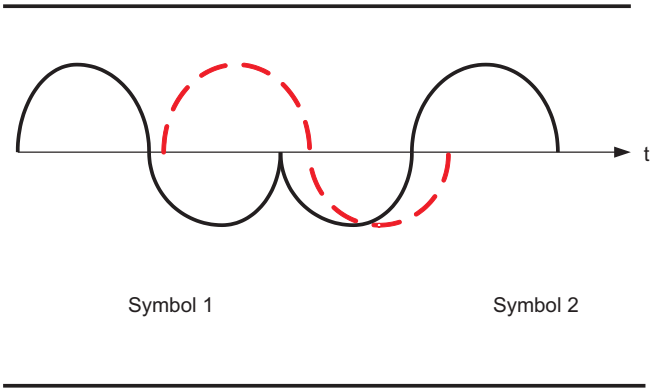

Figure 1.2: Delay from front symbol.

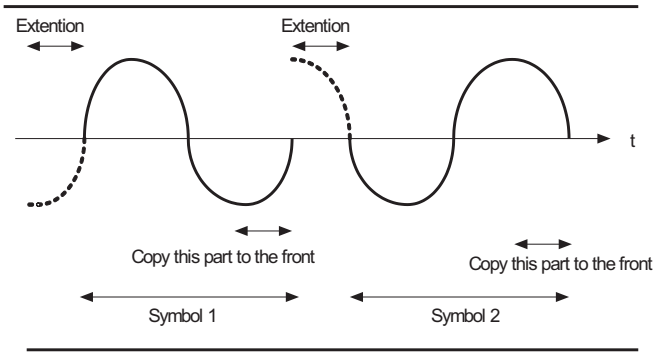

Figure 1.3: Cyclic prefix insertion.

Chapter 2

Wireless LAN According to IEEE 802.11p

2.1 Definition of Key OFDM Parameters

The IEEE 802.11p PHY has similar specifications as IEEE 802.11a with some changes. In IEEE 802.11p, a 10 MHz frequency bandwidth is used, instead of 20 MHz bandwidth in IEEE 802.11a, thus all parameters in the time domain for IEEE 802.11p are doubled compared with the IEEE 802.11a. The doubled guard interval reduces ISI more than the guard interval in IEEE 802.11a.

The IEEE 802.11p PHY uses 64 subcarriers OFDM that includes 48 data subcarriers and 4 pilot subcarriers. The 4 pilot signals are used for tracing the frequency offset and phase noise, and are located on subcarrier -21, -7, 7 and 21. The short training symbols placed at the first part of every data packet (t_1 through t_{10} shown in Figure 2.1), relates to the signal detection, time synchronization, and coarse frequency offset estimation. The long training symbols (T_1 and T_2), which are located after the short training symbols, are used for channel estimation. GI2 is used as guard interval for long training sequence and GI is used as guard interval for OFDM symbols .The cyclic prefix is employed to reduce the ISI.

The total training length is 16 μs. A short OFDM training symbol consists of 12 subcarriers, which are given by

$S_{-26,26} = \sqrt{(13/6)}\,\{0,0,1+j,0,0,0,-1-j,0,0,0,1+j,0,0,0,-1-j,0,0,0,$
$-1-j,0,0,0,1+j,0,0,0,0,0,0,0,-1-j,0,0,0,-1-j,0,0,0,1+j,0,0,0,1+j,$
$0,0,0,1+j,0,0,0,1+j,0,0\}$,

where the modulation is given by the element's value. The factor $\sqrt{(13/6)}$ is for normalizing the average power in the OFDM symbol. To improve the channel estimation accuracy, long OFDM training symbols are used. The long training symbols consist of 53 subcarriers that have a zero value at DC which are given by

$L_{-26,26} = \{1,1,-1,-1,1,1,-1,1,-1,1,1,1,1,1,1,-1,-1,1,1,-1,1,-1,1,1,$
$1,1,0,1,-1,-1,1,1,-1,1,-1,1,-1,-1,-1,-1,-1,1,1,-1,-1,1,-1,1,-1,1,$
$1,1,1\}$,

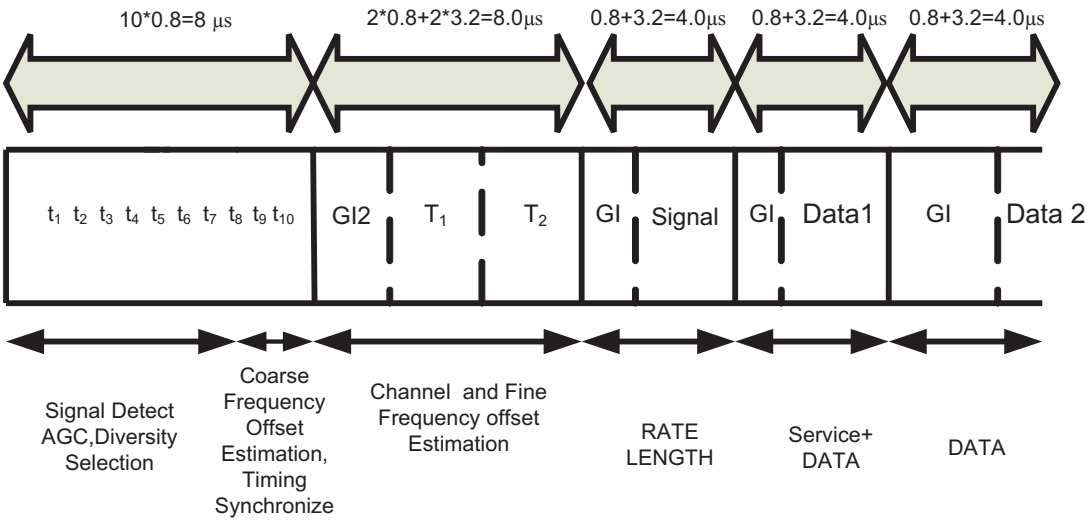

Figure 2.1: OFDM training structure.

where the modulation is given by the element's value. Depending on the data rates, different modulation schemes and coding rates must be applied. Table 2.1 illustrates the difference between IEEE 802.11p and IEEE 802.11a standard.

Table 2.1: Comparisons view on the key parameters of IEEE 802.11p PHY and IEEE 802.11a PHY (Source: [2])

Parameters	IEEE 802.11a	IEEE 802.11p
Bitrate Mb/s	$6, 9, 12, 18, 24,$ $36, 48, 54$	$3, 4.5, 6, 9,$ $12, 18, 24, 27$
Modulation Type	BPSK, QPSK, 16 QAM, 64 QAM	BPSK, QPSK, 16 QAM, 64 QAM
Code Rate	$1/2, 1/3, 1/4$	$1/2, 1/3, 1/4$
Number of Subcarriers	52	52
Symbol Duration	$4\,\mu$s	$8\,\mu$s
Guard Time	$0.8\,\mu$s	$1.6\,\mu$s
FFT Period	$3.2\,\mu$s	$6.4\,\mu$s
Preamble Duration	$16\,\mu$s	$32\,\mu$s
Subcarrier Frequency Spacing	0.3125 MHz	0.15625 MHz
Error Correction Coding	$K = 7$ (64 states) Convolutional Code	$K = 7$ (64 states) Convolutional Code

2.2 Definition of Physical Layer Coding

The messages are influenced by interference and in order to detect and correct the errors in received signals, the redundancy technique is introduced. For a binary

block code, an encoder is used in the transmission system to prepare data for transmission. A binary convolutional encoder is one kind of block code, which is used in the IEEE 802.11p standard. The coding rates of $R = 1/2, 2/3$, or 3/4, that correspond to the desired data rate had been used in 802.11 p. The convolutional encoder uses the generator polynomials $g_0 = 133$ and $g_1 = 171$ in octal mode. The constraint length of the encoder is 7 with bit rate 1/2. The bits denoted as "A" and "B" are output of the encoder. Puncturing is used to create higher data rates. Puncturing is a procedure through which the number of transmitted bits is reduced and the coding rate is increased. The puncturing patterns are described in section 3.1.2 and in detail in [7]. Figure 2.2 illustrates the convolutional encoder.

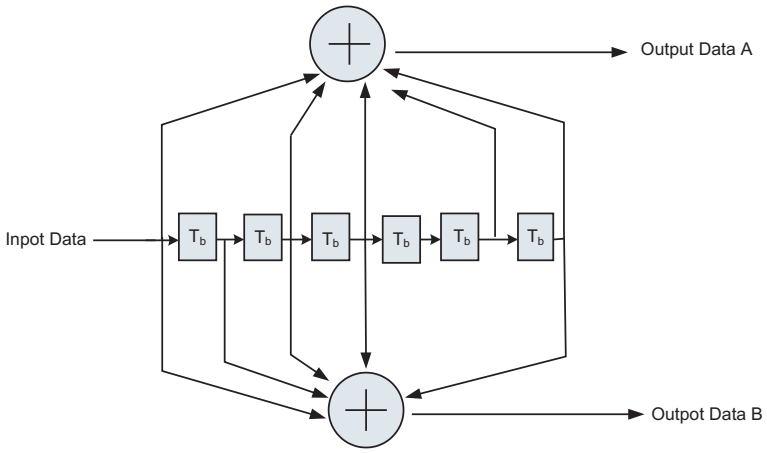

Figure 2.2: Convolutional encoder (k=7).

The minimum free distance of the code determines the performance of the convolutional code. d_{free} is the minimum Hamming distance between two different code words which is also called free distance.

2.3 Medium Access Control

The Medium Access Control (MAC) in IEEE 802.11p is the second layer of the lowest protocol layer of the network architecture based on the Open System Interconnection (OSI) model. Layer 2 is divided into two different sublayers, the logical link control (layer 2b), and the medium access control (layer 2a). The MAC is carried out to address some wireless communication events and control the medium access of the node, in order to reduce collisions. Because of medium access control, several stations can use the same physical medium. The basic access mechanism is called distributed coordination function.

2.3.1 The Basic Access Method

Distributed coordination function is basically a Carrier Sense Multiple Access (CSMA) in order to avoid collisions. To define the protocol, some acronyms must be introduced as follows:

- RTS: A station that wants to transmit a packet firstly transmits a short control packet that is called Request to Send (RTS). This packet is filled with information considering the source, destination, and duration of the transmission, [8].
- CTS: If the medium is free the destination station will respond with a control packet that is called Clear to Send (CTS), [8].
- IFS: Two Inter Frame Spaces IFSs (Distributed IFS and short IFS) are defined as time interval between frame, to present the delay between sending and receiving RTS, CTS, DATA and ACK packets, [9].
- ACK: An Acknowledgment (ACK) packet is sent from the receiver back to the transmitter mentioning the successful completion of the data exchange.

Figure 2.3 defineds a Carrier Sense multiple access protocol.

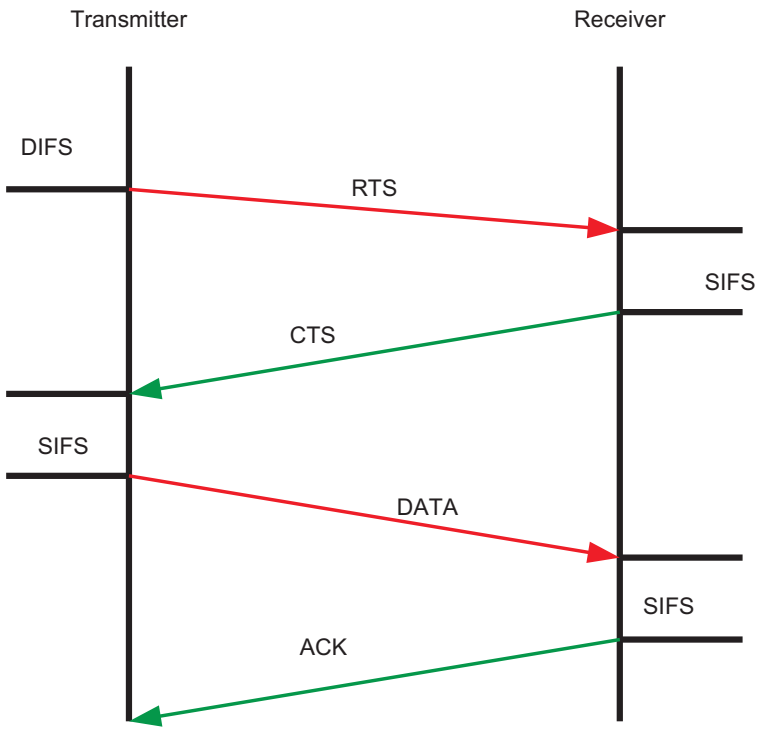

Figure 2.3: A CSMA protocol.

A CSMA protocol is implemented when a station willing to transmit a data packet. Since the medium is busy due to transmission of other stations, the station has to transmit the data packet to the receiver with a delay. This protocol

can be useful if the medium is not loaded heavily. Collision occurs when two or more stations transmit data at the same time . In order to overcome these problems, virtual carrier sense mechanism is defined as follows:

A station transmits a data packet, if the medium is free for a specified interval time (DIFS), then station decides to transmit a small packet (RTS). The receiver answers with a delay (SIFS time units), and sends a response to the source station as a small packet (CTS). The received CTS at source station shows that the receiver is ready to receive data. The source station will wait another SIFS unit and then sends the data packet. Once the receiver has received the data successfully, the receiver will wait SIFS units of time, and then send a response to source as a small packet called ACK. When the source receives ACK, it will be sure that the data exchange was successful. If the sender does not receive the ACK then it will continue transmitting the data until it gets a response. A station that receives one of these frames starts a timer, the Network Allocation Vector (NAV) which marks the medium as busy until the end of the protocol, [8].

2.3.2 Frame types

There are three main types of frames:

1. **Data frames**: Used for data transmission.
2. **Control Frames**: To address some wireless communication phenomena and control medium access of nodes in order to reduce collisions.
3. **Management Frames**: Are used to exchange management information, but they do not belong to the upper layers.

2.3.3 Most Common Frame Format

The Figure 2.4, 2.5 and 2.6 show some of the most common frames formats.

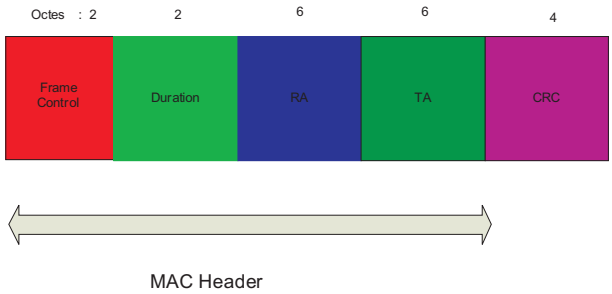

Figure 2.4: RTS frame format.

The frame control defines the type of frame (e.g. data frames, control frames and management frames) and depending on the frame type the duration is different. It can be the duration value that is used for NAV calculation as defined

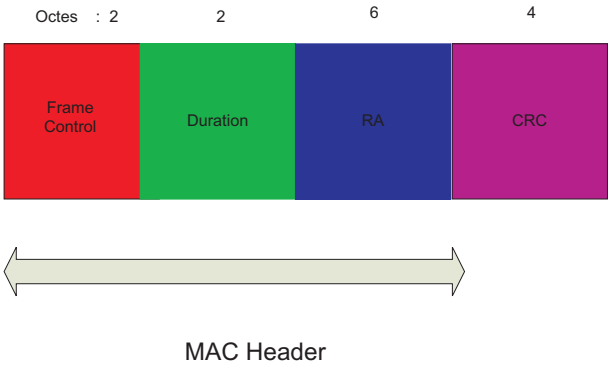

Figure 2.5: ACK frame format.

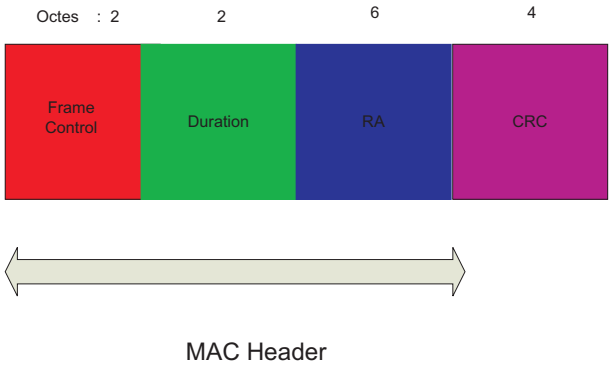

Figure 2.6: CTS frame format.

in the virtual carrier sense mechanism. RA and TA are the receiver address and transmitter address and CRC is used for cyclic redundancy check, [8].

Chapter 3

MATLAB/SIMULINK IEEE 802.11p Physical Layer Model

In order to develop the PHY of IEEE 802.11p, MATLAB SIMULINK is used. MATLAB has a large number of libraries and tool boxes, especially in the telecommunication field. I started from an available MATLAB/SIMULINK model, [1], according to IEEE 802.11a to obtain IEEE 802.11p PHY. The IEEE 802.11p model represents a baseband model for the physical layer in a Wireless Local Area Network (WLAN). Figure 3.1 illustrates the MATLAB/SIMULINK simulator architecture.

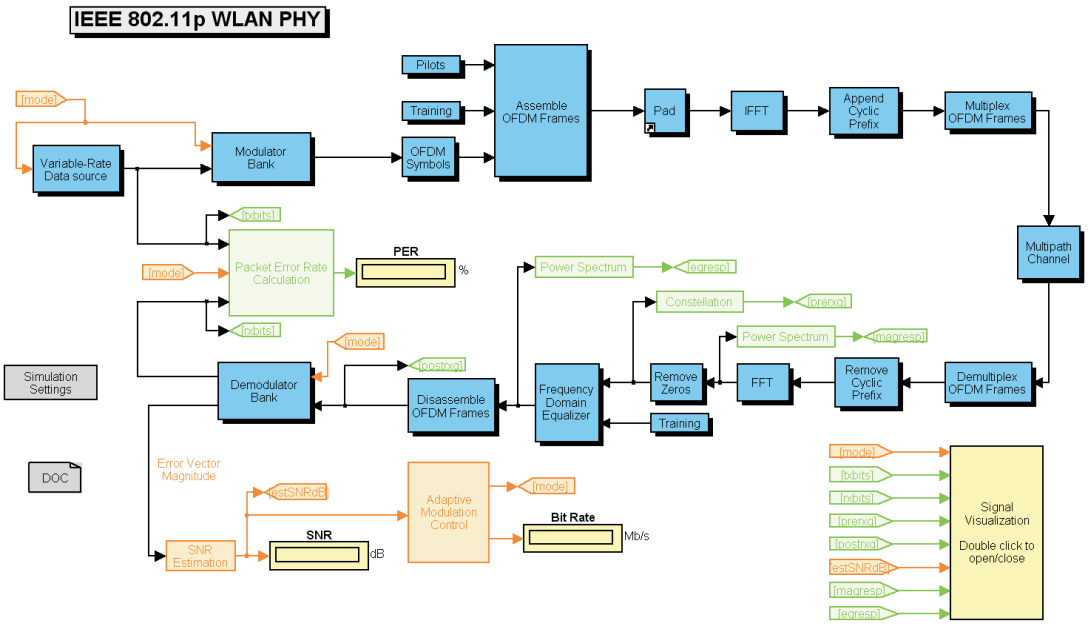

Figure 3.1: MATLAB/SIMULINK simulator architecture.

3.1 Transmitter Side

3.1.1 Variable-Rate Data Source

Binary data is created according to a predefined mode. This mode is created in adaptive modulation control according to the SNR estimation at the receiver. This mode has to be entered to the data source to create the binary data. In the subsystem of data source a buffer exists whose output is according to the maximum bits per block which are chosen in the simulation parameter list.

3.1.2 Modulator

IEEE 802.11p OFDM PHY includes different data rates which are selected according to the output of adaptive modulation. The system uses different modulation schemes due to different data rates. Figure 3.2 illustrates the subsystem of modulator. The modulator is subdivided as following:

- Padding
- Convolutional encoder
- Puncturing convolutional codes
- Matrix interleaver
- General block interleaver
- Rectangular QAM

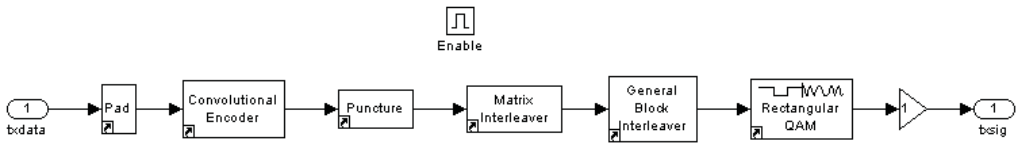

Figure 3.2: Subsystem of modulator.

Padding

The Padding block changes the dimension of input matrix along its columns, rows or both of them according to the specified values. In this system each row is equal to one subcarrier, it means, rows are in the frequency domain and columns are in the time domain. In IEEE 802.11p baseband model the padding is employed for truncating the input signal along column size. The specified output dimension is the number of bits per block that is different according to the different data rate and corresponding different code rate and modulation scheme.

Convolutional Encoder

A convolutional encoder is carried out for coding of the transmitted bits. Convolution codes have three main parameters, the number of input bits, k, number of output bits, n, and the number of memory register, m. $k.(m+1)$ is introduced as constraint length to define a convolutional encoder in Matlab Simulink. A *poly2trellis* function is used to convert generator polynomials to Trellis structure, see [10].

$Trellis = poly2trellis$(Constraint Length , Code Generator)

In this system the Trellis structure is *poly2trellis* $(7, [171\,133])$.

Puncturing Convolutional Codes

Generation of different code rates from 1/2 code rate, which is the code rate of the convolution encoder, is implemented through puncturing. The output elements will be according to the puncture vector. The k^{th} element of the input vector will be removed if the k^{th} element of puncture vector is zero. On the other hand if the k^{th} element of puncture vector is equal to one, then the k^{th} element of the input vector is represented in the output vector. The following example illustrates creating new code rates from 1/2 code rate:

To create a 3/4 code rate from a 1/2 code rate, one convolutional code with one puncture vector $[110110]$ and constraint length 7 can be used. The third and sixth element from the input vector are removed according to the puncture vector. Therefore the bit rate resulting from puncture vector is 3/2, finally bit rate will be $3/4 = 3/2.1/2$, [11].

Matrix Interleaver and General Block Interleaver

Interleaving can be employed in digital data transmission technologies to mitigate the effect of burst errors. When too many errors exist in one code word, due to a burst error, the decoding of a code word can not be done correctly. To reduce the effect of burst error, the bits in one code word are interleaved before being transmitted. When interleaving occurs the place of bits will change, which means that a burst error can not disturb a huge part of one code word. Figure 3.3 illustrates the effect of interleaving at the transmitter.

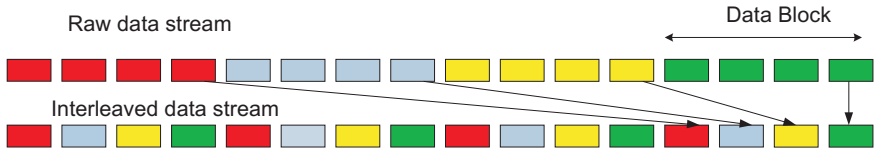

Figure 3.3: Transmission with interleaving.

This example explains that only a small part of each code word is distorted with interleaving, so the decoding of code word can be done correctly. The interleaving

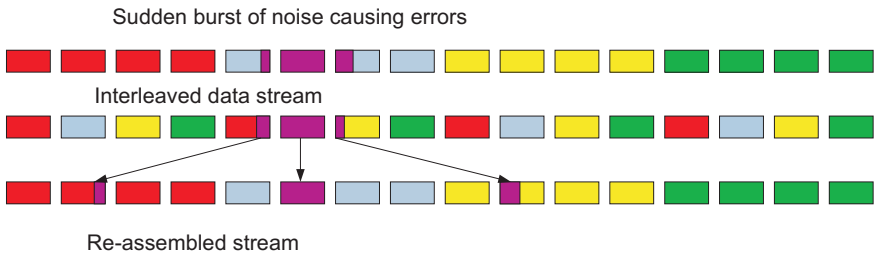

Figure 3.4: Transmission with a burst error and interleaving.

in this SIMULINK model is defined by two steps. The first step is mapping of the adjacent coded bits into the nonadjacent subcarriers that is implemented with the matrix interleaver. The second step is mapping the adjacent coded bits alternately onto significant bits of the constellation that is implemented with the general block interleaver.

Matrix interleaver interleaves the input vector according to the specified row and column. In this system the number of rows and columns is given by:

Interleaver Rows = 16

Interleaver Columns = Number of transmitted bits per block / interleaver Rows

Figure 3.5 illustrates an example of the current process of the matrix interleaver block. The input vector is a column vector. The dimensions of input vector in matrix interleaver convert to a 2 by 3 matrix. The first three elements of input vector are the first row of matrix and the second three elements of input vector are the second row of matrix. Finally the matrix interleaver block rewrites the elements column by column. Therefore the first two elements of output are the first column of matrix, the second two elements of output are the second column and the third two elements of output are the third column.

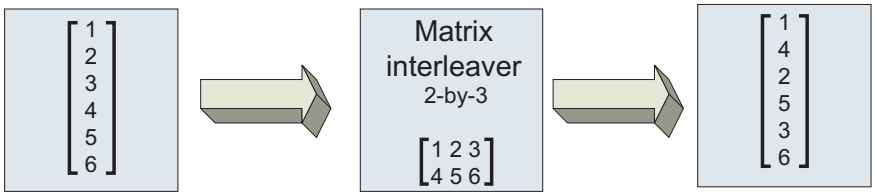

Figure 3.5: Matrix interleaver.

The second step of interleaving is implemented with the general block interleaver that changes the place of input elements according to the elements vector. According to the elements vector, the first element of output is the forth element of input, the second element of output is the first element of input, the third element of output is the third element of input and the fourth element of output is the second element of input. Figure 3.6 explains this process.

The parameters of the matrix and general block interleaver of the IEEE 802.11p baseband model are following the standard, defined in [7].

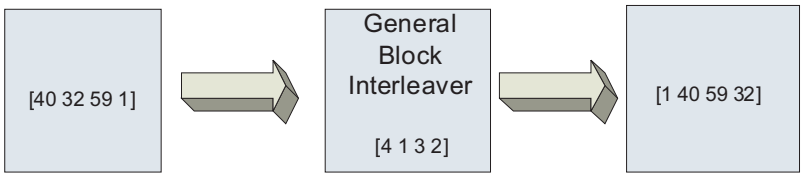

Figure 3.6: General Block interleaver.

Rectangular QAM

The rectangular QAM block is applied to indicate how the binary words are assigned to points of the signal constellation. In the IEEE 802.11p baseband model a Gray-code is used. Four different modulation types are implemented:

- BPSK
- QPSK
- 16 QAM
- 64 QAM

3.1.3 OFDM symbols

To convert a block of N serial data symbols (each has a duration of T_s) into a block of N parallel data symbols (each has a duration of $T = NT_s$), the modulator is using a reshape block. The output vector is a number of data subcarriers by OFDM symbol per frame.

3.1.4 Pilot insertion

Each OFDM symbol in IEEE 802.11p has four pilot subcarriers. The pilot signals are used for tracing frequency offset and phase noise. The location of pilot subcarriers is -21,-7, 7 and 21.

The Pseudorandom Noise (PN) sequence generator block is carried out creating the pilot subcarriers. The sample time and the number of samples per frame for PN sequence Generator is defined as follow:
Sample time = the period of the Block/OFDM symbol per frame
Samples per frame = OFDM symbol per frame

3.1.5 Preamble

Preamble insertion is used for channel estimation in our model in order to improve the channel estimation accuracy. Four long OFDM training symbols are used instead of two long training symbol in this system. The long training symbols consist of 53 subcarriers that have a zero value at DC subcarrier. The long training symbol is defined in 2.1.

3.1.6 Assemble OFDM Frames

The assemble OFDM frames is applied in order to insert the pilot and training symbols into the OFDM symbols. Figure 3.7 shows the subsystem of this block. Four pilots are inserted between the subcarriers and then training sequence is added to the subcarriers.

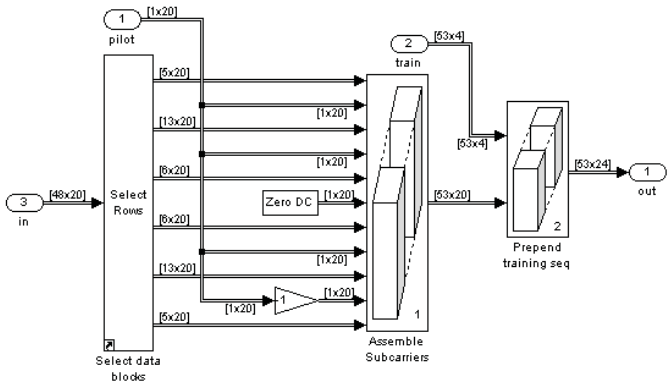

Figure 3.7: Assemble OFDM frame subsystem.

3.1.7 Padding

The Pad block extends the input vector along its columns. The padding values are equal to zero, inserted at the end of the columns, where the specified dimension of the output is the number of points of the IFFT block.

3.1.8 IFFT and FFT

An inverse Fourier transform converts the frequency domain data stream into the corresponding time domain. Then a parallel to serial convertor is used to transmit time domain samples of one symbol. The Fast Fourier Transformation (FFT) is used to convert data in time domain to the frequency domain at the receiver. The serial to parallel block convertor is placed to convert this parallel data into a serial stream to obtain the original input data. Figure 3.8 illustration the process.

IFFT block allocates the different orthogonal subcarrier for transmitted bits and thus no interference exists between subcarriers. In this situation sub-carriers can be closer together, which means that bandwidth can be saved significantly, [11].

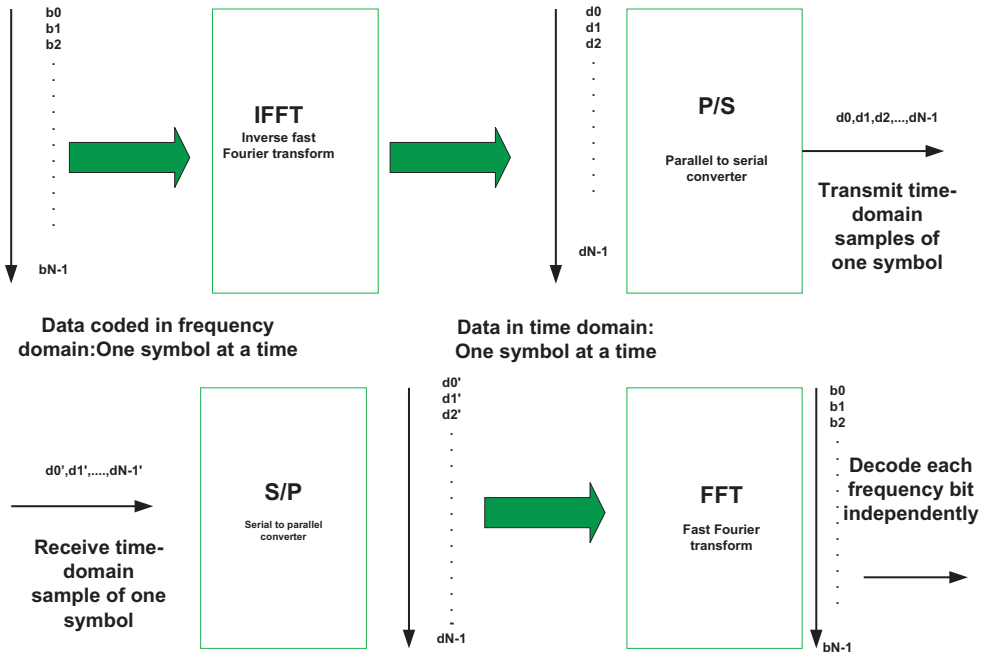

Figure 3.8: IFFT/FFT description.

3.1.9 Cyclic Prefix

Cyclic prefix is used as a guard interval to mitigate the effect of ISI due to the multipath propagation. A selector block is applied as a cyclic prefix inserter to insert the last 16 subcarriers into the beginning of the OFDM symbols.

3.1.10 Multiplex OFDM Frame

The multiplex block is the last block in the transmitter part to convert the signal from parallel to serial and to transmit time-domain samples of one symbol.

3.2 Radio Channel

For the first simulation a simple Additive White Gaussian Noise (AWGN) channel model is used, following by simulations with multipath Rayleigh fading together with AWGN model. In order to get a more realistic channel model for vehicular scenarios, we use a specific channel simulator called WinProp.

3.2.1 AWGN Channel

To implement the effect of AWGN on the input signal, an AWGN channel is added to the input signals. This block produces a complex output signal when the input signal is complex. In this model the variance is specified from the port

that inserts SNR, in order to calculate the variance of the noise, as shown in Figure 3.9, [12].

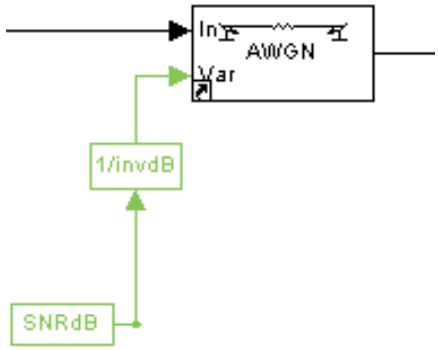

Figure 3.9: AWGN channel.

3.2.2 Rayleigh Fading Channel with AWGN

The multipath Rayleigh fading is added to an AWGN channel. Since a transmitted signal propagates along several paths in multipath channel to reach to the receiver, it may lead to different time delays. In the block, two parameter dialogs are specified, the delay vector is used to specify time delay for each path and the gain vector is used to specify the gain for each path at each delay. The number of paths is according to the length of the delay vector and the gain vector which must have the same length.

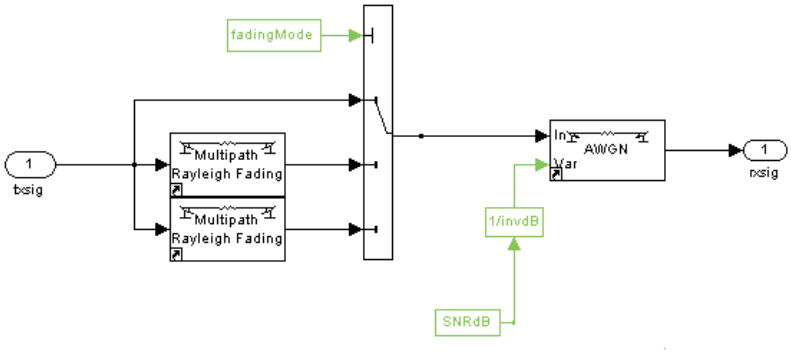

Figure 3.10: Multipath Rayleigh fading channel.

3.2.3 Advanced Model Using WinProp Simulator

WinProp [3] is a Software package for the simulation of electromagnetic waves and radio systems in static and time variant environments. The channel from the WinProp simulations is used instead of the simpler model (Rayleigh fading and AWGN) in order to achieve more realistic results. Low cost and fast determination of a channel impulse response, and creating the scenarios easily are some advantages of WinProp simulator.

WinProp-Time Variant scenarios

In this section a short introduction to the time variant usage of WinProp is given. The introduction explains that the software package can be used for predictions in time variant scenarios, [13].

To create a realistic channel for V2V communication with WinProp , the following steps can be passed:

1. StreetMan is used to create road courses.
2. WallMan is used to create additional objects (buildings, cars,...) and setting the time variant properties of the objects.
3. ProjectMan is used to create a project with all settings related to the computation (transmitter, receiver, result,...).
4. SiMan is used for the computation in time variant scenarios.
5. ProMan is used for visualization of prediction results.

Figure 3.11 illustrates the process for the creation and simulation of a new scenario.

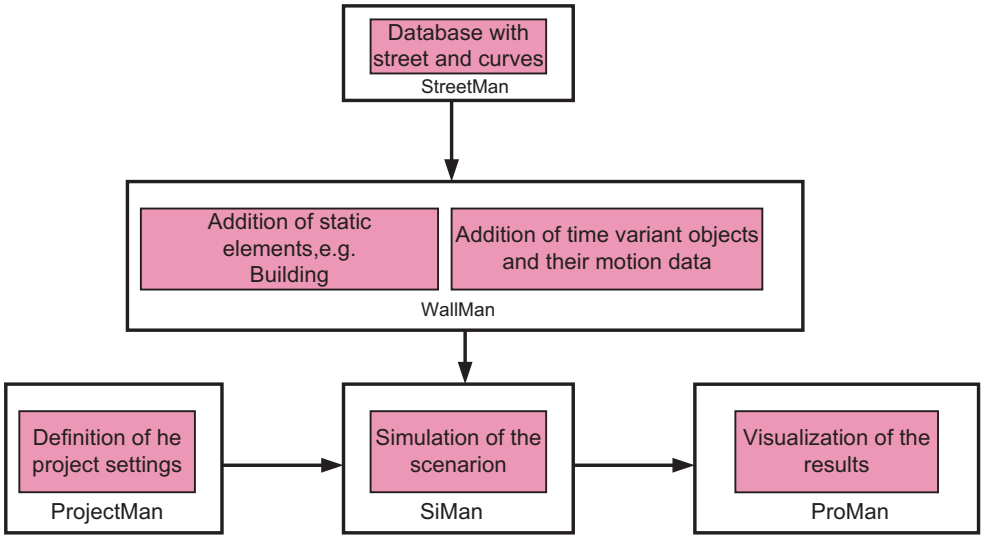

Figure 3.11: Process for the creation of a time variant scenario.

ProjectMan is applied to create a project, where some properties like transmit power, center frequency, antenna pattern and antenna placement of transmitter

are defined. In addition the properties of receiver like antenna pattern and antenna placement are defined in ProjectMan. The number of snapshots, type of polarization, and type of output files after simulation are other properties that are defined in ProjectMan. SiMan is used for the computation time variant scenarios. After finishing the simulations, the results appear as different file formats:

- cir file: Channel impulse response
- fpf file: Field strength result
- fpp file: Power result file
- fpl file: Path loss result file
- str file: Propagation paths for visualization in ProMan
- mat file: A specific MATLAB output

The mat file contains the impulse response matrix of the channel and it contains following variable:

- Matrix
- Date
- Delta delay
- Frequency
- Maximum delay
- Minimum delay
- Power
- Snapshots
- Time

The elements of the matrix are field strength in μV/m. Minimum delay, maximum delay and delta delay (resolution) are in ns, center frequency is in MHz and transmit power is in dBm. Also mat file contains the date and time of creation of mat file.

The following steps describes the implementation of the channel from the mat file into the SIMULINK PHY model.

1. Using the digital filter to convolve the transmit signal with the channel matrix to obtain the output signal. The convolution for continuous time can be expressed by, [4],

$$y(t) = \int_{-\infty}^{\infty} x(t-\tau)h(t,\tau)d\tau. \tag{3.1}$$

   $x(t)$= Input signal
   $y(t)$= Output signal
   $h(t)$= Channel impulse response

2. Setting the digital filter to the FIR filter

Finite Impulse Response (FIR) digital filter operates by convolving the input signal $x(n)$ with the filter's impulse response $h(n)$ to find the output signal as described in Figure 3.12, [14].

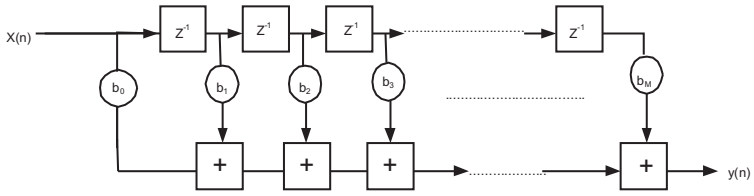

Figure 3.12: FIR filter.

$x(n-k)$ is the input with a delay equal to k, where $k = 0, 1, 2, \cdots, M$ and

$$y(n) = b_0x(n) + b_1x(n-1) + b_2x(n-2) + b_3x(n-3) + ... + b_Mx(n-M)$$
$$= \sum_{m=0}^{M} b_m x(n-m) = \sum_{m=-\infty}^{\infty} h(m)x(n-m) = (h * x)(n) \quad (3.2)$$

3. Specifying FIR filter as time varying filter

   The coefficients of time variant filter change with time. In this model a time varying filter is used that the coefficients of filter change once per input frame. The second input port of the FIR filter is used for the insertion of the channel impulse responses as coefficients of the filter. The input of this port can not be a matrix, therefore the channel matrix is converted with a buffer block to a column vector, to obtain a frame based input for the FIR filter.
4. Adding AWGN to the output of the time variant filter.
   .

3.3 Receiver Side

3.3.1 Demultiplex OFDM Frame

To convert a signal from serial to parallel, a demultiplex block is used. A reshaping block is a subsystem of this block and is employed to produce a matrix out of the input vector.

3.3.2 Remove Cyclic Prefix

In the receiver the inserted cyclic prefix must be removed, to obtain the original input data. A selector block is used to remove the 16 subcarriers that are inserted into the beginning of the OFDM symbols.

3.3.3 FFT

A FFT block computes the fast Fourier transformation (FFT) along each column for all input matrices to convert a time domain signal to frequency domain.

3.3.4 Frequency Domain Equalizer

To restore the transmitted signal, a zero-forcing equalizer is used that applies the inverse of the channel frequency response. The combination of channel and zero forcing equalizer output gives a flat frequency response with linear phase to obtain the transmitted signal, [5]. Figure 3.13 illustrate a zero-forcing equalizer. $F(f)$ is channel frequency response and C(f) is inverse of the channel frequency response.

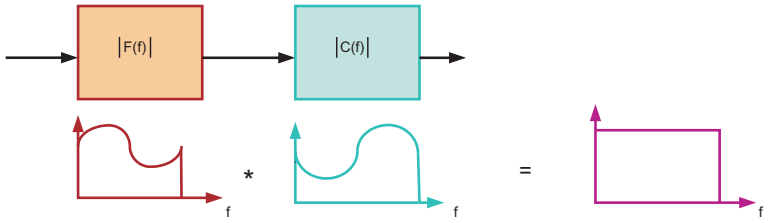

Figure 3.13: Zero-Forcing equalizer.

The frequency domain equalizer block has two input signals, the training symbols, which are also used at the transmitter, and the received symbols. As depicted in Figure 3.14, the received signal is splitted up into the training symbols and data symbols. The channel estimation is done by dividing the received training symbols through the true training symbols. This estimation is used for the zero-forcing equalizer. The subsystem of the equalizer gaing is shown in Figure 3.15.

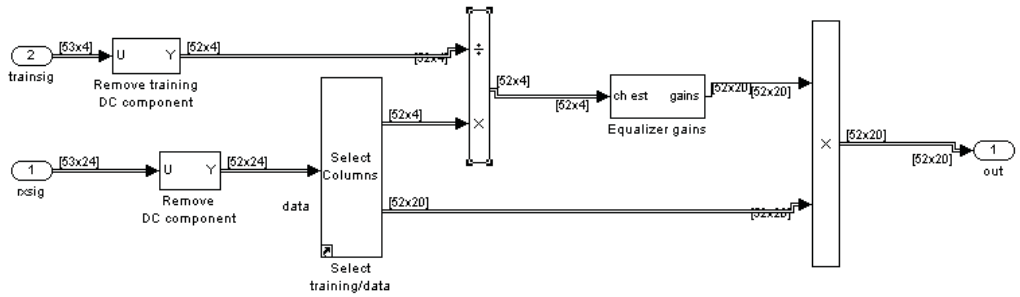

Figure 3.14: Subsystem of equalizer.

The estimated channel is the input of the equalizer gain block and the output is the inverse of the channel estimation. According to the zero-forcing equalizer

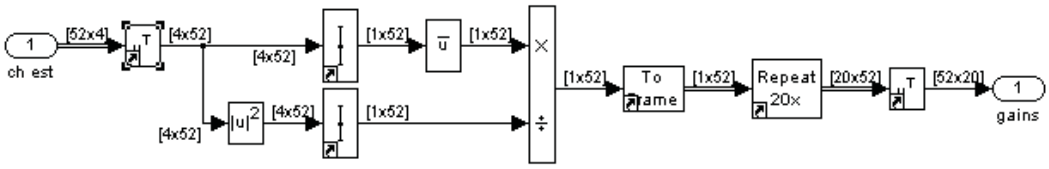

Figure 3.15: Subsystem of equalizer gains.

technique with combination of received data and zero forcing equalizer output (inverse of channel estimation), the estimated signal before the channel can be achieved.

3.3.5 Disassemble OFDM Frame

In this part the data subcarriers are separated from pilot subcarriers and the N parallel data symbols are converted to the N serial data symbols, to achieve the original signal.

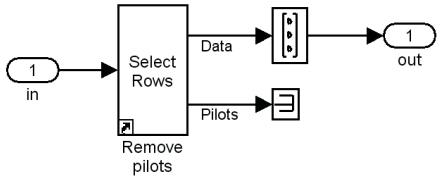

Figure 3.16: Disassemble OFDM frame.

3.3.6 Demodulator Bank

The demodulator subsystem performs the inverse tasks of the modulator subsystem. Figure 3.17 illustrates the subsystem of demodulator bank.

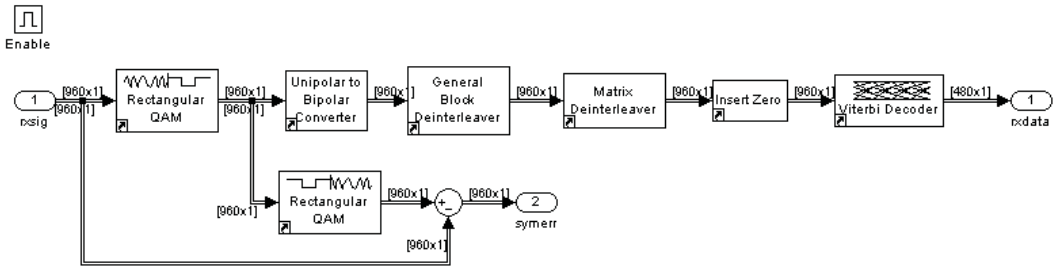

Figure 3.17: Subsystem of demodulator bank.

Zero insertion

The opposite of puncturing is zero insertion. With the puncture vector at the transmitter, different code rates were created and at the receiver a zero insertion block is used to convert the code rates to the base code rate, 1/2. The following example determines the inverse process of puncturing.

If the input vector is [1 3 4 5 7 9 10 11] and the insert zero vector parameter be a vector like [1 0 1 1 1 0], the input vector will be divided into two groups, each with four elements. This happens because of there are four elements one in the insert zero vector. Based on this, the block inserts zeros after the first and last elements of each group of four elements. This results in a 2/3 code rate. If the code rate of the encoder is 3/4, the code rate after the insert zero block is 1/2 = 2/3.3/4. The Figure 3.18 explains this process.

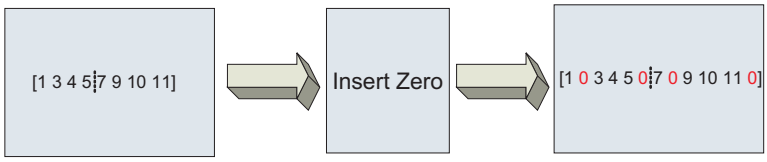

Figure 3.18: Zero insertion.

Viterbi decoding

The Viterbi decoder block works according to the maximum likelihood decoding. It means finding the most probable transmitted symbol stream from the received code word.

The Viterbi decoder, [4], defines a metric for each path and makes a decision based on this metric. The most common metric is the Hamming distance metric. When two paths come together on one node, the shortest hamming distance is kept. The number of trellis branches is defined as trace back depth that is 32 in this model.

To define a convolution decoder in MATLAB simulation a *poly2trellis* function is used to covert convolution code to trellis description, [10].

$trellis$ =$poly2trellis(ConstraintLength$, $CodeGenerator)$

In this system trellis structure is $poly2trellis$[7,[171 133]].

3.3.7 Adaptive Modulation Control

Adaptive modulation systems improve the rate of transmission. The implementation of adaptive modulation is according to the channel information that is present at the transmitter. The method of making adaptive modulation in this model is according to the estimated SNR, a bit rate will be specified and then data source generates binary data according to the specified data rate in adaptive modulation control.

3.3.8 Evaluation of Reliability Modules

Bit Error Rate

The error rate calculation block calculates the bit error rate, by comparing the received data with transmitted data.

It has three inputs, T_x and R_x port that are used to accept transmitted and received signals and the third port is used to indicate the related frame for computation.

Packet Error Rate

In this block the numbers of errors in the packet will be divided by the number of packets for the calculation of packet error rate. Packet error rate is taken over the last 50 frames.

Chapter 4

Definition of Vehicular Scenarios

The radio propagation characteristics are determined by many factors, such as operating frequency band, signal bandwidth, time variant properties of objects and antenna characters. Therefore we define two V2V scenarios, which were simulated with the simulation tool WinProp, in this section is detail. In both scenarios the antennas are placed on the top of the vehicles and an isotropic radiator is assumed for the transmit and received antennas. In scenario I the cars are going in opposite directions and in scenario II the cars are going in the same direction around a corner.

4.1 Scenario I: Cars Are Going in Opposite Directions

In this scenario the transmitter- and receiver-car are going in opposite directions. Further there is a third car, a truck, which is going ahead the receiver car. The transmitter-car is a orange sedan and the receiver-car is a blue transporter. In order to simplify the scenario there is no building next to the road, only a guard rail and the street are modelled. There is one lane in each direction. Figure 4.1 depicts this scenario. The complete scenario is defined with following parameters:

Transmitter:

- T_x power: 18 dBm
- Center frequency: 5.9 GHz
- Antenna pattern: Isotropic
- Antenna placement: Roof of the car
- Polarization: Vertical
- Height of the antenna: 1.5 m
- Car type: Sedan (blue)
- Car speed: 15 m/s

Receiver:

- Antenna pattern: Isotropic

- Antenna placement: Roof of the car
- Polarization: Vertical
- Height of the antenna: 1.5 m
- Car type: Transporter (orange)
- Car speed: 15 m/s

Environment and other cars:

- One lane in each direction
- Straight street
- Guard rails along the street
- Third car (truck) ahead the receiver-car with speed 10 m/s

In order to define the number of snapshots in time, the following settings have to be specified. The start time, end time and interval time (time resolution). The interval time shall be equal to the frame length of the SIMULINK PHY model, which is $24 \times 8\mu\,s = 192\mu\,s$. The start time is equal to 0 s and end time is equal to 5 s. Further the minimum delay, maximum delay and delay resolution has to be set. The delay resolution is equal to the inverse of the signal bandwidth, which is 10 MHz in IEEE 802.11p. The maximum delay is equal to the time interval.

- Minimum delay: 0 ns
- Maximum delay: 10000 ns
- Delay resolution: 100 ns

4.2 Scenario II: Cars Are Going in the Same Direction

In this scenario the transmitter- and receiver-car are going in the same direction. One further car is going into the opposite direction. There are several buildings next to the street, see Figure 4.2. As in Scenario *I* there is one lane per direction and a guard rail is along the street. The street is not straight as in Scenario *I*, but there is also one curve. The complete scenario is defined with following parameters:

Transmitter:

- T_x power: 18 dBm
- Center frequency: 5.9 GHz
- Antenna pattern: Isotropic
- Antenna placement: Roof of the car
- Polarization: Vertical
- Height of the antenna: 1.5 m

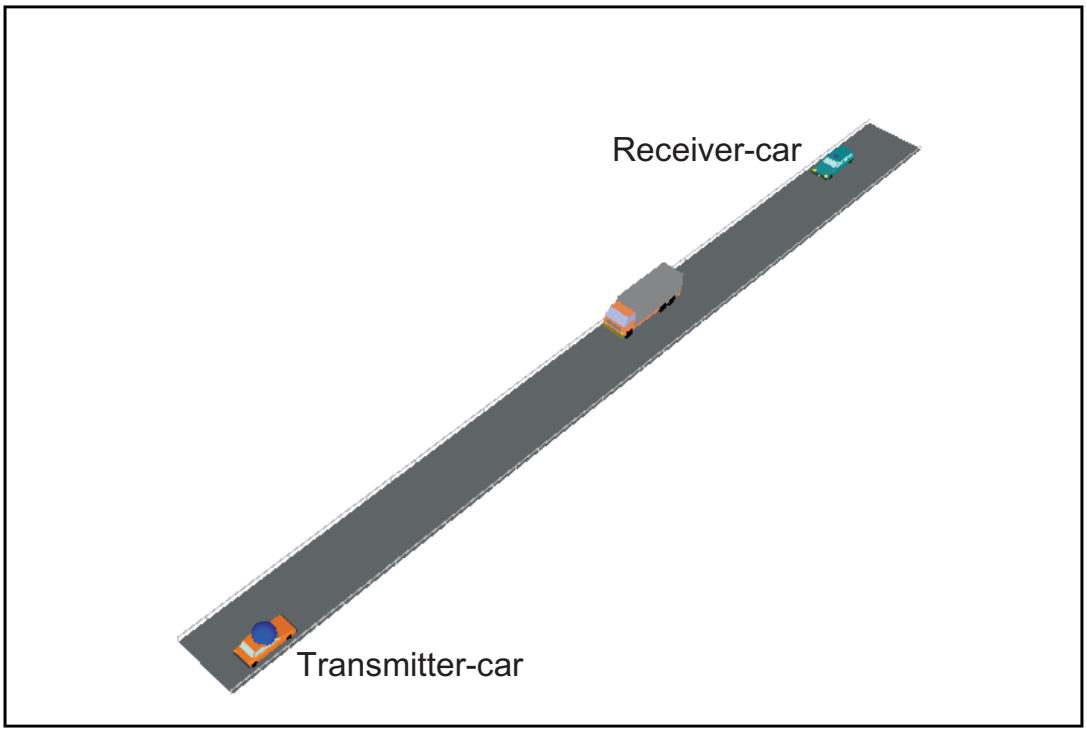

Figure 4.1: Vehicular scenario I .

- Car type: Sedan (blue)
- Car speeds: 10 m/s, 11 m/s, 12 m/s and 13 m/s are related to the distance 0 m, 25 m, 53.50 m and 65 m respectively

Receiver:

- Antenna pattern: Isotropic
- Antenna placement: Roof of the car
- Polarization: Vertical
- Height of the antenna: 1.5 m
- Car type: Transporter (orange)
- Car speeds: 14 m/s, 10 m/s, 10 m/s and 10 m/s are related to the distance 0 m, 40 m, 68.50 m and 81 m respectively

Environment and other cars:

- One lane in each direction
- Street with one curve
- Guard rails along the street
- Seven buildings next to the street
- Third car is going in opposite direction with speeds: 12 m/s, 10 m/s, 10 m/s and 15 m/s are related to the distance 0 m, 7.20 m, 15.50 m and 49 m respectively

The time and delay paramters are the same as in Scenario I.

- Start time: 0 s
- Stop time: 5 s
- Time interval: 192 μs
- Minimum delay: 0 ns
- Maximum delay: 10000 ns
- Delay resolution: 100 ns

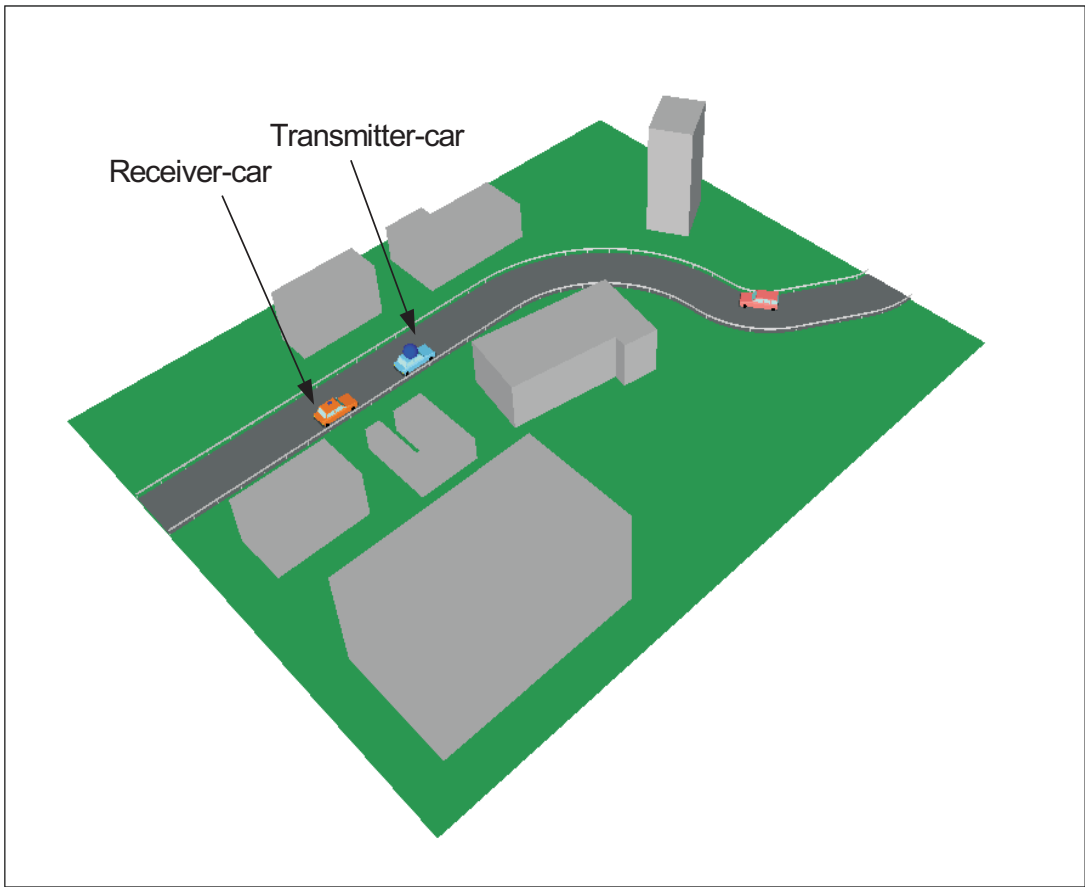

Figure 4.2: Vehicular scenario II .

Chapter 5

Discussion of Simulation Results

5.1 Simulation Result of AWGN Channel

In this part the comparison of simulation result with a theoretical curve of error probability for distinct modulation schemes, BPSK and QPSK is discussed. In physical layer investigation of the IEEE 802.11p standard, the BER versus SNR can be the reference for the whole vehicular wireless network.

The theoretical bit error probability ,P_b, for uncoded BPSK is, [15],

$$Pb = Q\left(\sqrt{\frac{2E_b}{N_0}}\right). \tag{5.1}$$

In this formula E_b is the bit energy, N_0 is the noise power spectral density and Q(x) is defined by

$$Q(x) = \frac{1}{2} erfc\left(\frac{x}{\sqrt{2}}\right). \tag{5.2}$$

The first step of comparison the SIMULINK results with theoretical error probability is for the validation. For validation of results a correcting factor is used, in order to reflect the cyclic prefix and pilot-carriers, which are carrying no information. Because of that, a part of energy of a transmitted OFDM symbol is lost, [15].

The correcting factor for BPSK can be expressed as 80/64 that is added to the SNR in order to obtain E_b/N_0. Figure 5.1 illustrates a comparison of simulation result and theoretical curve of error probability for BPSK modulation with an AWGN channel. The vertical axis shows the bit error probability and horizontal axis shows the E_b/N_0. In general, the higher the E_b/N_0, the fewer the errors probability in the simulation results. The BER versus E_b/N_0 for the 3 Mbps data rate (BPSK modulation scheme with 1/2 coding rate) and theoretical curve are close together, which validates our simulations.

Figure 5.2 shows the PER versus E_b/N_0 plot for QPSK modulation with 1/2 coding rate. The PER for simulation results is more than 0.5 at 5 dB E_b/N_0, and followed by a moderate drop to obtain a low value of PER in larger than 7.5 dB

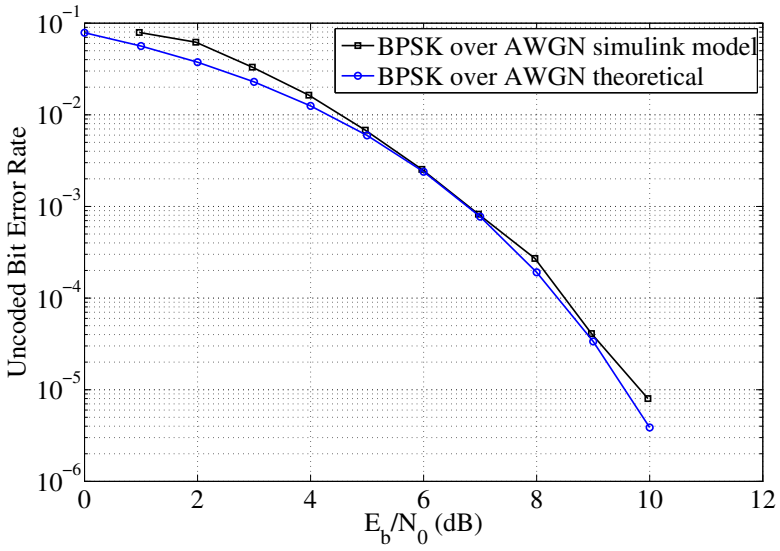

Figure 5.1: Error probability for BPSK modulation scheme.

E_b/N_0. The PER for simulation results in [2] illustrate that PER is more than 0.5 at 5 dB E_b/N_0 and is followed by a moderate drop to obtain a low value of PER in 10 dB E_b/N_0. Comparison between simulation results for PER over 2304 last frames and simulation result in [2] demonstrates that in both two cases the values of PER is decreasing in the duration between 5 dB E_b/N_0 until more than 7.5 dB E_b/N_0,which validates our simulations.

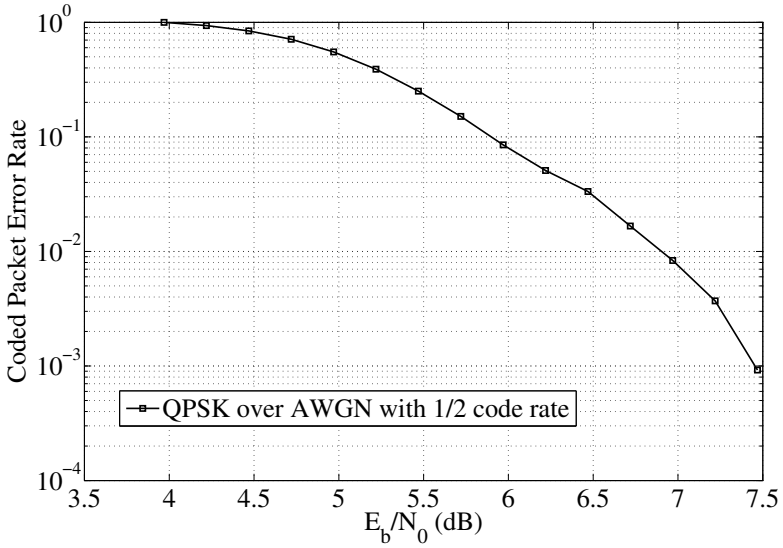

Figure 5.2: Packet error probability for QPSK modulation scheme.

5.2 Simulation Result of a Multipath Rayleigh Fading and AWGN Channel

In this part the comparison between simulation results and theoretical error probability is shown. A Rayleigh fading channel with AWGN for uncoded transmission is considered. Furthermore QPSK modulation scheme with 1/2 coding rate is used as modulation technique.

The correcting factor in this case is the same as for BPSK , see section 5.1, and the number of tap delay is 1 and maximum delay is 100 ns.

Figure 5.3 demonstrates the simulation result of a QPSK modulation with 1/2 coding rate over a AWGN and fading channel. The start point of simulation result curve is BER of 0.5 at −30 dB SNR for the QPSK modulation. This is followed by a slight drop in 0 dB SNR. BER continues to fall moderately until 30 dB SNR, when a low values of BER is obtained. Furthermore Figure 5.3 illustrates the simulation result of a QPSK modulation over a AWGN and fading channel is matched with theoretical curve, which validates our simulations.

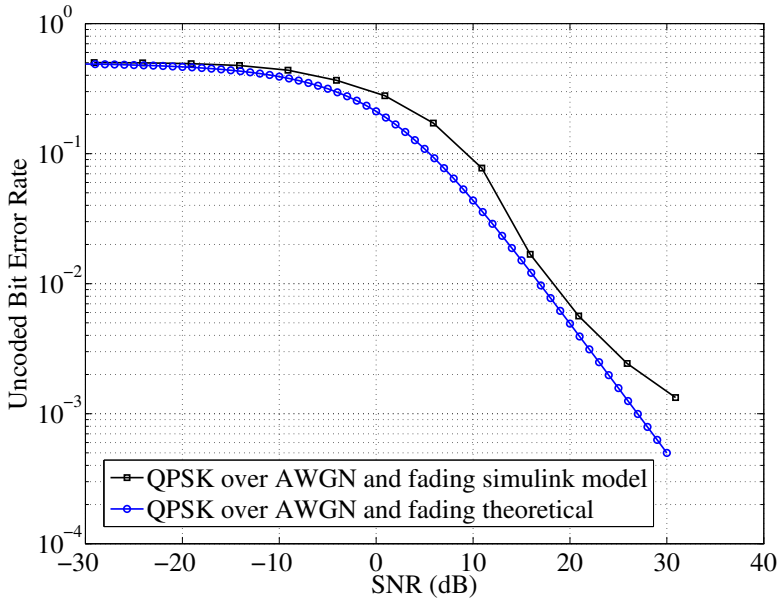

Figure 5.3: Error probability for BPSK modulation scheme.

Bit error probability ,P_b, for QPSK modulation scheme is given by equation ,[16],

$$Pb = \frac{1}{2}\left(1 - \frac{\mu}{\sqrt{2-\mu^2}}\right)\sum_{k=0}^{K}\binom{2k}{k}\left(\frac{1-\mu^2}{4-2\mu^2}\right)^k, \tag{5.3}$$

where K is the number of bit symbol and μ is

$$\mu = \sqrt{\frac{SNR}{1 + SNR}}. \tag{5.4}$$

5.3 Comparison between Coded and Uncoded AWGN Channel

Figure 5.4 shows the BER performance versus E_b/N_0 of the coded and uncoded transmission over an AWGN channel for BPSK modulation scheme. The start point of BER versus E_b/N_0 for uncoded transmission is BER of 0.024 at 1 dB E_b/N_0. The BER is decreasing moderately until 5 dB E_b/N_0, when BER reaches to 7×10^{-3}. The start point of the BER versus E_b/N_0 for coded transmission is BER of 0.079, which is 5% less than uncoded transmission. BER for uncoded transmission continues to fall sharply in comparison with coded transmition. BER for uncoded transmission at 2.5 dB E_b/N_0 is 4.5×10^{-2} and BER for coded transmission at 2.5 dB E_b/N_0 is 5.5×10^{-4} which demonstrate the provment of BER over coded transmission. Figure 5.4 describes that the simulation results with coding have lower error compared with the simulation results without coding, because of error detection and correction with convolutional encoder.

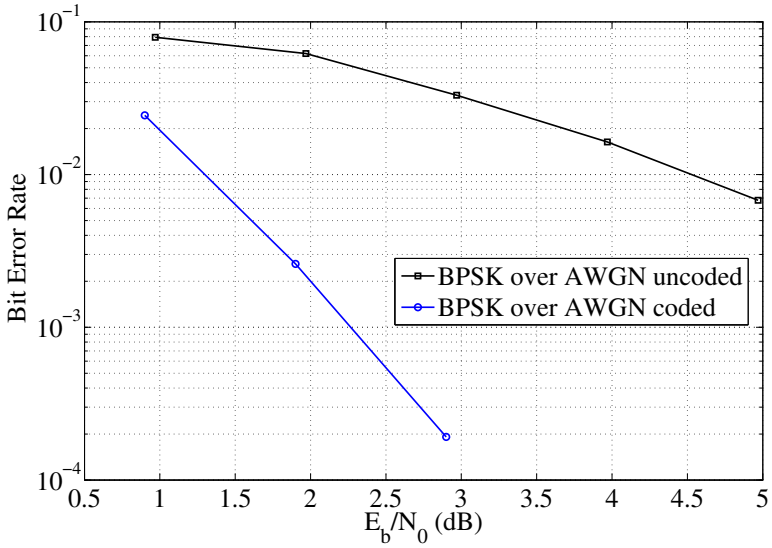

Figure 5.4: Bit error probability for BPSK modulation scheme.

5.4 Packet Error Rate Calculation

Figure 5.5 and 5.6 show the PER performance versus SNR of the coded and uncoded transmission over 50 last frame. The higher the SNR, the fewer the PER

in the simulation results. Furthermore comparison between Figure 5.5 and 5.6 illustrates that coded transmission has lower PER compared with the simulation results for uncoded transmission.

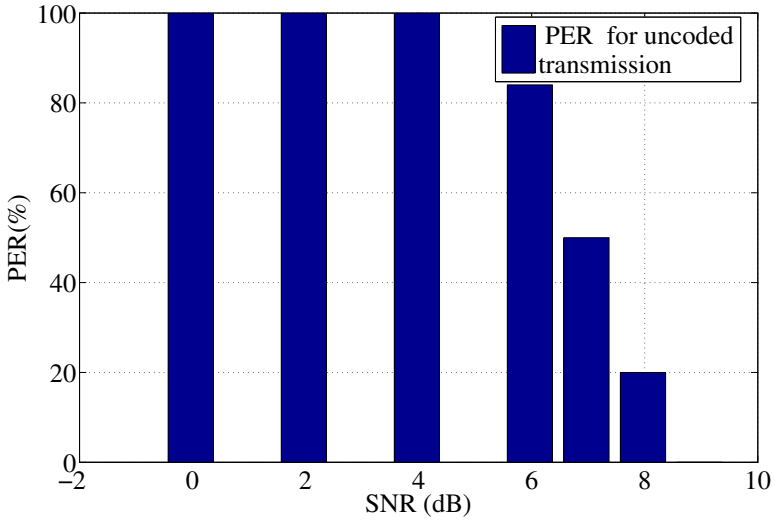

Figure 5.5: Packet Error Rate of BPSK over AWGN channel.

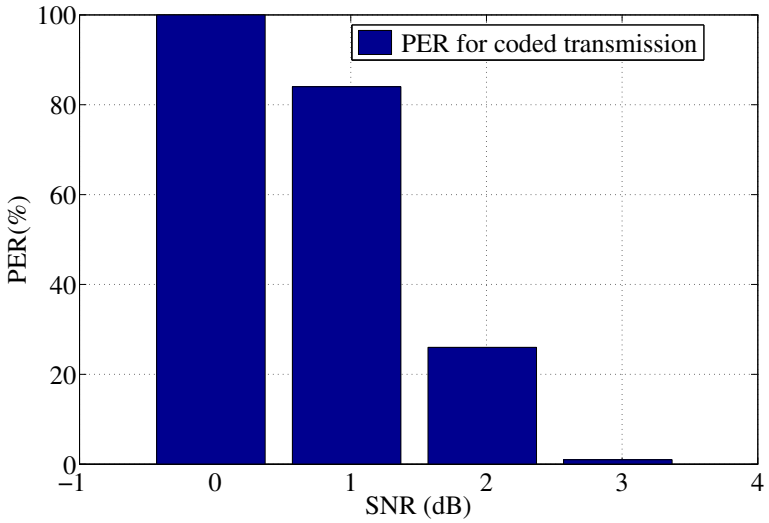

Figure 5.6: Packet Error Rate of BPSK over AWGN channel.

5.5 Simulation Result of Multipath Rayleigh Fading and AWGN Channel with Different Tap Delay

Since in the multipath channel signals are reflected at multiple places, they reach the receiver from several different paths that may have different lengths and different corresponding time delays. To specify the channel with different tap delays in fading channel a tap-model is used which is called ITU vehicular channel A [17]. This model is not allocated to V2V communication, this is a Channel impulse response model based on a tapped-delay. The model is specified by the number of taps, the time delay relative to the first tap and the average power relative to the strongest tap. The model is set up according to the Table 5.1.

Table 5.1: ITU Vehicular Channel Model (Channel A)(Source: [17])

Tap	**Relative delay(ns)**	**Average power(dB)**
1	0	0.0
2	310	-1.0
3	710	-9.0
4	1090	-10.0
5	1730	-15.0
6	2510	-20.0

The comparison of BER for simulation results for vehicular channel A and QPSK over AWGN and fading SIMULINK model is illustrated in the Figure 5.7. The correcting factor is the same as before. Simulation results in this part are somewhat different which is due to more than one tap delay in vehicular channel A.

Maximum excess delay in vehicular channel is $2.510\mu\,s > 1.6\mu\,s$ (cyclic prefix) the RMS delay spread and mean excess delay are 604.1 ns and 466.10 ns. The RMS delay spread in this case is less than cyclic prefix.

Mean Excess delay and RMS delay are,[5],

$$\text{Mean Excess Delay} = \frac{\sum_{k=0}^{K} p(\tau_k).\tau}{\sum_{K0}^{k} p(\tau_k)} \tag{5.5}$$

$$\text{RMS delay} = \sqrt{(\overline{\tau^2}) - (\overline{\tau})^2} \tag{5.6}$$

$$\overline{\tau^2} = \frac{\sum_{k=0}^{K} p(\tau_k)\tau_K^2}{\sum_{k=0}^{K} p(\tau_k)} \tag{5.7}$$

where K is number of paths.

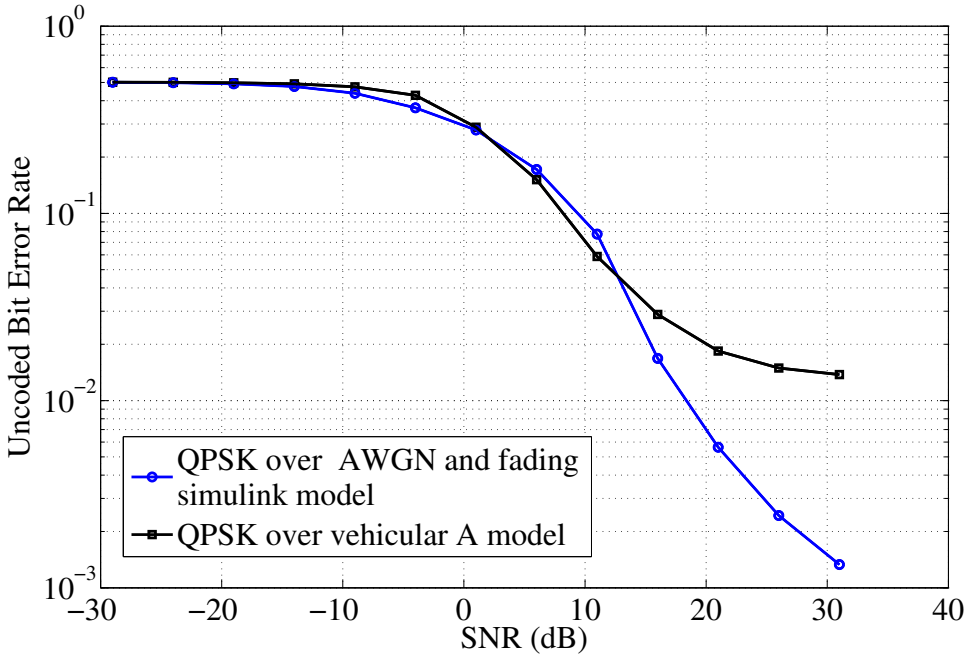

Figure 5.7: Error probability for QPSK modulation scheme.

5.6 Advanced Channel Model using WinProp

The channel resulting from WinProp is used in the SIMULINK model instead of the simpler model,mention in the last sections, to achieve more realistic results. Distinct vehicular scenarios described in section 4 are used in this part.

The resolution of the delay is defined according to the Tx sample rate in Matlab simulation that is 100 ns. In this part the normalization of impulse response matrix is taken into account to obtain more realistic result. Equation 5.8 define the relation between transmit signal and received signal,

$$Y = (H * X) + N, \tag{5.8}$$

equation 5.9 is used to define a certain value of SNR. To simplify obtaining the SNR, the values of mean power ($E\{|H(x)|^2\}$) and Average transmit power ($E\{|x|^2\}$) is set to one,

$$SNR = \frac{E\{|H(x)|^2\}}{E\{|N|^2\}}.E\left\{|x|^2\right\}, \tag{5.9}$$

Therfore

$$SNR = \frac{1}{E\{|N|^2\}}. \tag{5.10}$$

Equation 5.11 and Equation 5.12 are the definition of mean power,[4],

Continuous:

$$MeanPower = lim_{T\to\infty}\frac{1}{T}\int_{-T/2}^{T/2}\int_{0}^{\infty}|h(t,\tau)|^2 d\tau dt, \tag{5.11}$$

Discrete:

$$MeanPower = lim_{T\to\infty}\frac{1}{T}\sum_{h=-k}^{k}\Delta t\sum_{l=0}^{L}|h(k\Delta t, l\Delta t)|^2\Delta\tau, \tag{5.12}$$

in MATLAB the impulse response channel matrix is divided to square root of mean power to normalize the $(E\{|H(x)|^2\})$ to one.

Simulation Result of Advance Channel Model in Opposite Direction

The MATLAB output of WinProp contains the field strength in $\mu V/m$ in three components, E(x), E(y), and E(z). Figure 5.8 illustrates the magnitude of E(z) as a function of time. Due to the vertical polarization the magnitude of E(z) is more than the magnitude of E(x) and E(y). Figure 5.8 illustrates that the magnitude of E(z) is increasing until two cars reaching to each other at $t = 2.9\,\mathrm{s}$. The magnitude is decreasing due to the increasing the distance between two cars after passing from each other.

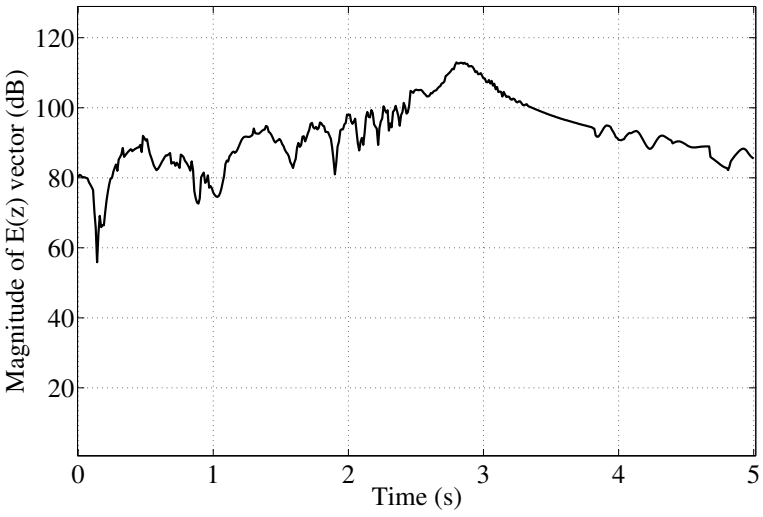

Figure 5.8: Magnitude of E(z) vector (dB).

Figure 5.9 shows the BER for vehicular scenario in opposite direction. The comparison between Figure 5.8 and Figure 5.9 illustrates that when a fading accrues, the magnitude of E(z) vector is decreasing and the bit error rate is increasing. When two cars reach to each other, the highest values of magnitude

for E(z) occurs, and therefore a decreasing of values for BER are obtained. Then the values of BER increase due to the increasing the distance between two cars after passing from each other. Figure 5.10 shows the different values of data rate that generated according the adaptive modulation.

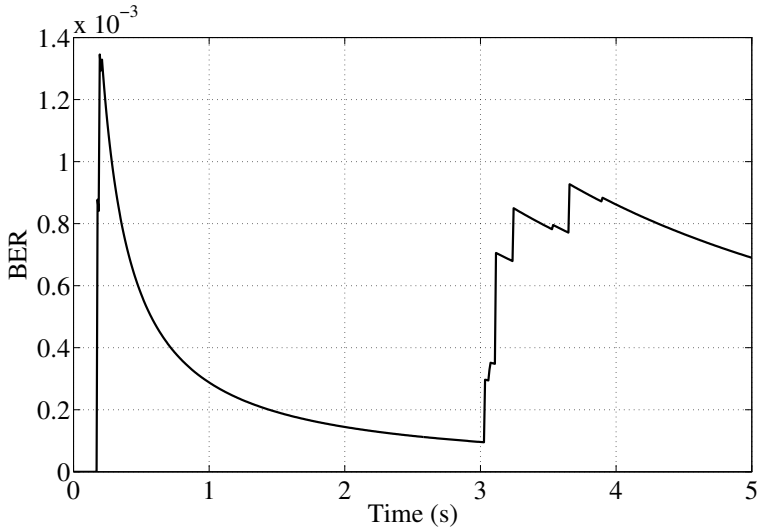

Figure 5.9: BER of vehicular scenario in opposite direction.

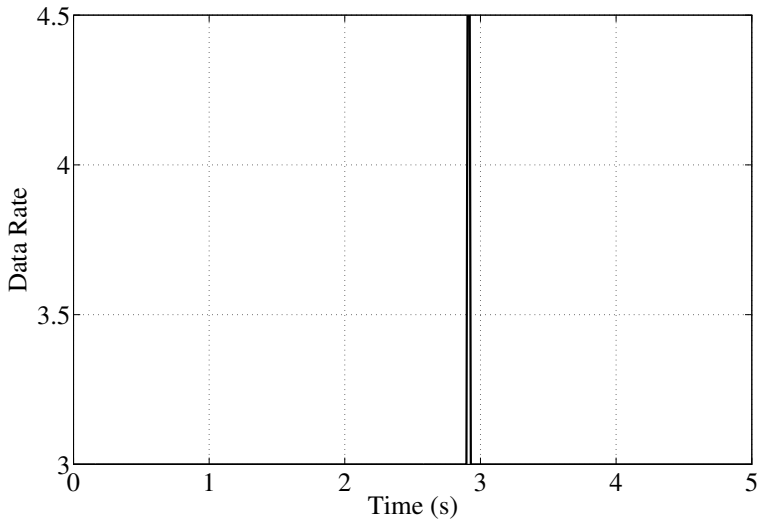

Figure 5.10: Data rate of vehicular scenario in opposite direction .

Simulation Result of Advance Channel Model in Same Direction

Figure 5.11 illustrates the magnitude of E(z) as a function of time. Due to the vertical polarization the magnitude of E(z) is more than the magnitude of

E(x) and E(y). The magnitude of E(z) is changing between 95 dB to 105 dB in the same direction of transmitter and receiver scenario. The curve of E(z) in the same direction scenario is varying less than variation in opposite direction scenario, because of the higher variation of the Doppler shift in the opposite direction scenario. The magnitude of E(z) decreases at $t = 3.7$ s, when the third car is passing from the transmitter and receiver in the opposite direction. Figure 5.12 shows the BER for vehicular scenario in the same direction. The comparison between Figure 5.11 and Figure 5.12 illustrates that when the third car is passing from the transmitter and receiver, the lowest values of magnitude for E(z) occurs, and therefore an increasing of values for BER are obtained. Figure 5.13 shows the different values of data rate that generated according to the adaptive modulation.

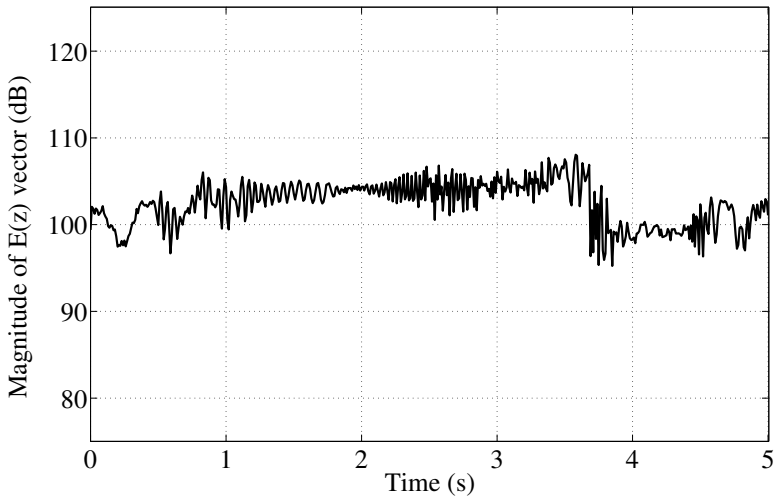

Figure 5.11: Magnitude of E(z) vector (dB) .

Analyzing of received power for Advance Channel Model

Figures 5.14 and 5.15 illustrate the received power and pathloss related to the transmitter that is on the roof of the orange car was showed in figure 4.1. Received power is decreasing by distance and will not be understandable in blue area due to sensitivity level of ITS transceivers in practice.

The Path loss is increased by distance. In the near area to the transmitter, we can see that pathloss is less than 60 dB and it is increasing to more than 100 dB in higher distances. This phenomenon is illustrated in Figure 5.15.

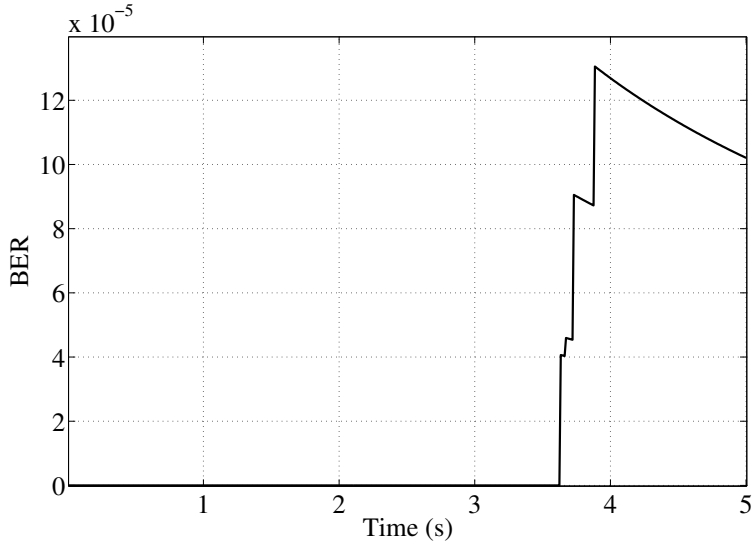

Figure 5.12: Bit error rate of vehicular scenario in same direction .

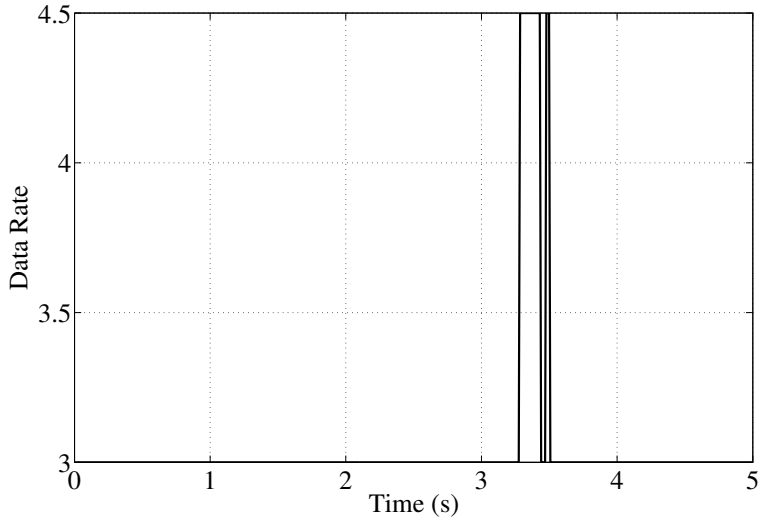

Figure 5.13: Data rate of vehicular scenario in same direction .

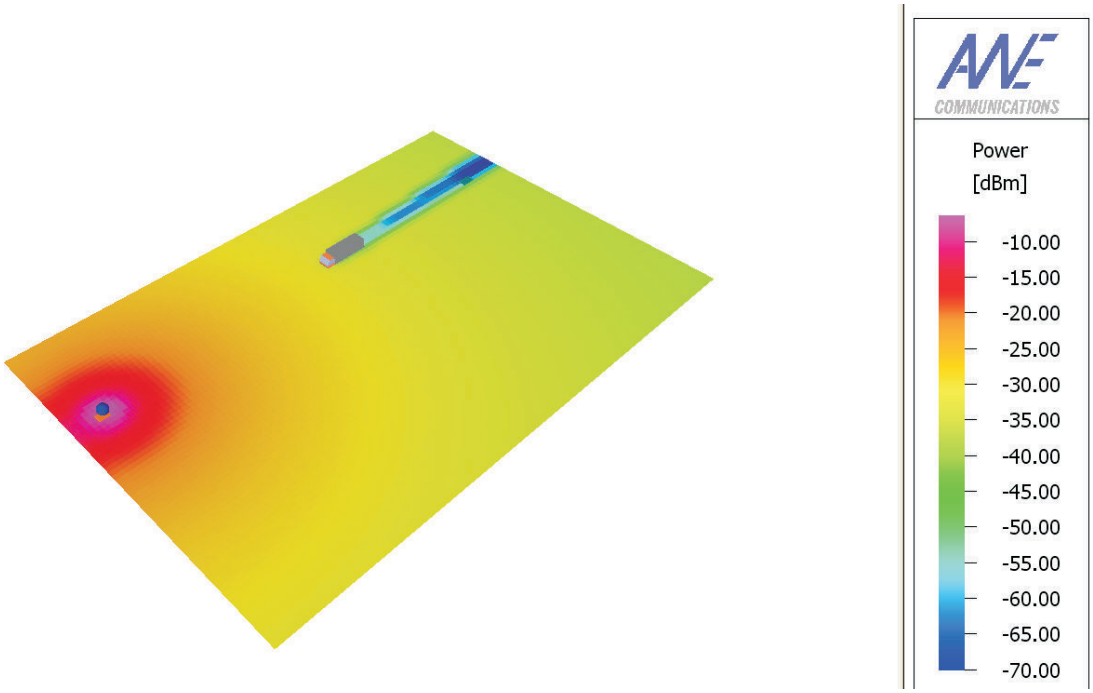

Figure 5.14: Received power.

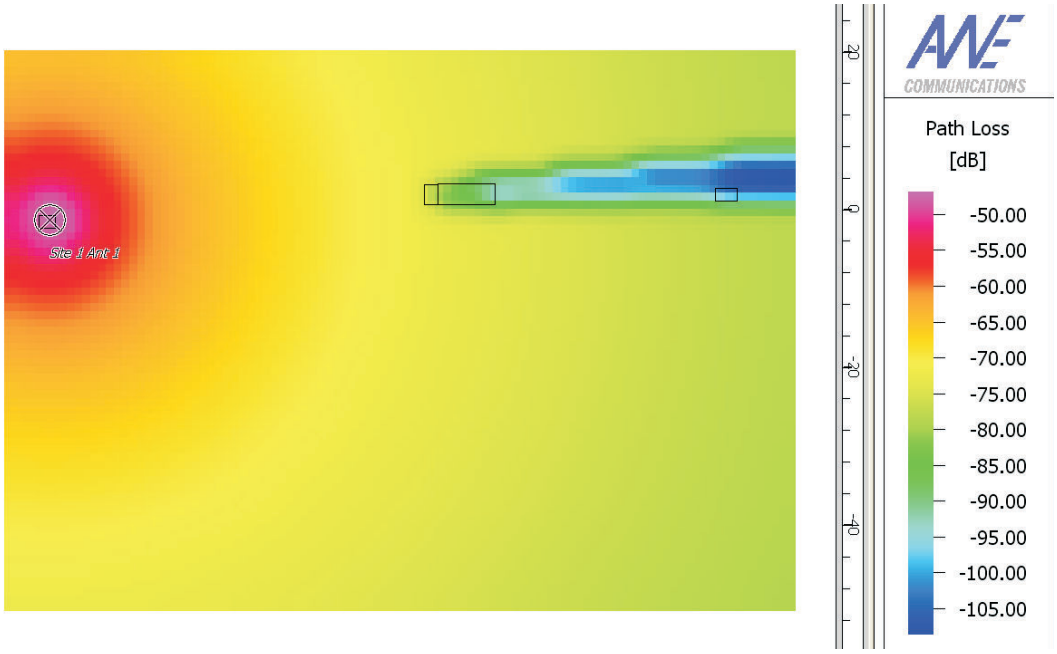

Figure 5.15: Path loss.

Chapter 6

Conclusions

At this work a MATLAB simulation was carried out in order to analyze baseband processing of the proposed IEEE 802.11p physical layer. Different channel implementations are used for the simulations. For the first simulation a simple AWGN channel model is used, following by simulations with multipath Rayleigh fading together with AWGN model. In order to get a more realistic channel model for vehicular scenarios, I use a specific channel simulator called WinProp. The WinProp is a Software package for the simulation of electromagnetic waves and radio systems in static and time variant environments.

I compared my simulation results with theoretical curves of error probability to validation of my simulation result. The comparison of BER versus E_b/N_0 for AWGN channel and theoretical curve illustrate that simulation result over BPSK modulation scheme with 1/2 coding rate are close together. The comparison of simulation results over Rayleigh fading and AWGN channel with theoretical curve for QPSK by 1/2 coding rate illustrates that the simulation results and theoretical curve are matched together, which validates our simulation results.

I have integrated a ray-tracing based software tool, WinProp, for modelling time variant vehicular channel into SIMULINK. Normalization of impulse response matrix is taken into account to obtain more realistic results. The comparison between the simulation results of advanced channel model using WinProp in same direction scenario and opposite direction scenario illustrates that the curve of E(z) in the same direction scenario is varying less than variation in opposite direction scenario. Furthermore the value of BER for vehicular scenario in same direction is less than the values of BER for vehicular scenario in opposite direction because of the higher variation of the Doppler shift in the opposite direction scenario.

A description of the principles of the IEEE 802.11p PHY and working experience with MATLAB SIMULINK and WinProp software was obtained through this thesis.

Bibliography

[1] http://www.mathworks.com/matlabcentral/fileexchange/3540, M. Clark, "IEEE 802.11a WLAN model."

[2] Y. Zang, L. Stibor, G. Orfanos, S. Guo, and H. Reumerman, "An error model for inter-vehicle communications in highway scenarios at 5.9 GHz," in *International Workshop on Modeling Analysis and Simulation of Wireless and Mobile Systems*, Montreal, Quebec, Canada, 2005.

[3] http://www.awe com.de/Automotive/, AWE Communications GmbH.

[4] A. F. Molisch, *Wireless Communications*. IEEE-Press - Wiley and Sons, 2005.

[5] T. S. Rappaport, *Wireless Communications: Principle and Practice*. NJ: Prentice-Hall, 1996.

[6] E. Limpert, W. A. Stahel, and M. Abbt, "Log-normal distributions across the sciences: Keys and clues," *Bio Science*, vol. 51, pp. 341–352, 2001.

[7] IEEE 802.11, "Wireless LAN medium access control (MAC) and physical layer (PHY) specifications," June 2003.

[8] P. Brenner, "A technical tutorial on the IEEE 802.11 protocol," Breezecom Wireless Communications, July 1996.

[9] P. Pant and T. Castelli, "Simulation of a wireless network using the 802.11 MAC protocol," Final Report.

[10] www.mathworks.com/access/helpdesk/help/toolbox/commblks, communications blockset, Convolutional encoder.

[11] L. Z. Fuertes, "OFDM PHY layer implementation based on the 802.11a standard and system performance analysis," B.Sc. thesis, 2005, university of Linköping, Linköping, Sweden.

[12] www.mathworks.com/access/helpdesk/help/toolbox/commblks, communications blockset, AWGN channel.

[13] R. Wahl, "An introduction to WinProp time variant," AWE Communications GmbH.

[14] H. Monson, *Statistical Digital Signal Processing and Modeling*. Wiley, 1996.

[15] E. Mark, *Wireless OFDM Systems: How to Make Them Work?* Kluwer Academics Publishers, 2002.

[16] J. G. Proakis, *Digital Communications*. McGraw-Hill, 1995.

[17] TU-R Rec. M 1225, "Guidelines for evaluation of radio transmission technologies (RTTs) for IMT-2000," 1997.

List of Figures

List of Tables